



Quark gluon plasma in an early phase of the Universe and in the laboratory

J. Milošević

University of Belgrade and
Vinča Institute of Nuclear Sciences,
Belgrade, Serbia



28.08.2020

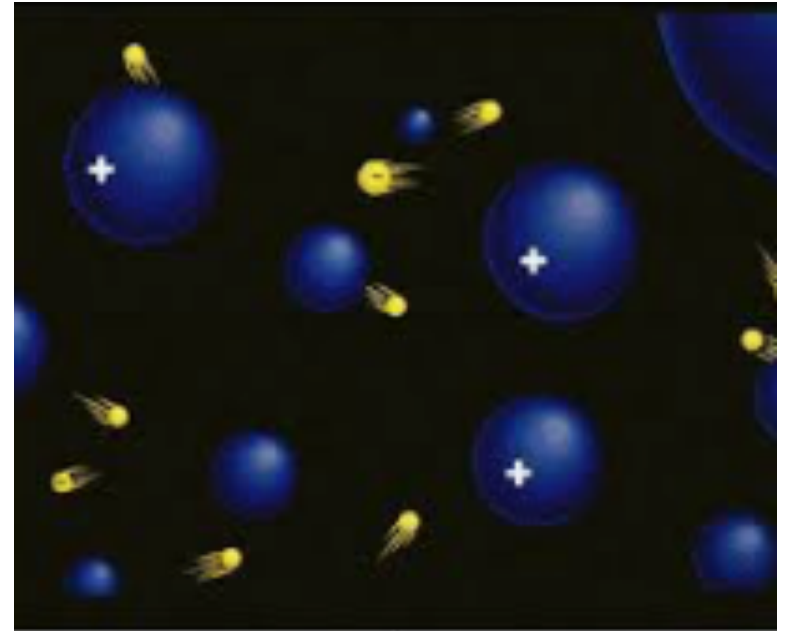
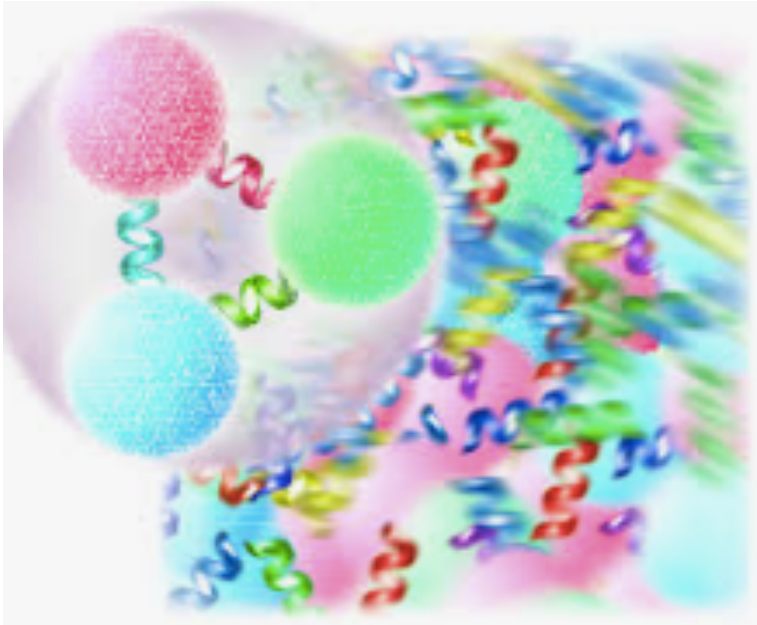
30th SPIG

1

Outline

- ❖ Quark Gluon Plasma (QGP) as a system of deconfined quarks and gluons (partons)
 - ✧ Similarities and differences wrt electromagnetic (EM) plasma
- ❖ T - μ_B phase diagram of nuclear matter
- ❖ QGP in the early Universe and in the laboratory nucleus-nucleus (AA), proton-nucleus (pA) and proton-proton (pp) collisions
 - ✧ Similarities and differences between the early Universe and QGP formed in the laboratory
- ❖ Some of the QGP signatures
 - ✧ Jet (spray of hadrons) suppression
 - ✧ Collective movements of partons (particle anisotropy)
- ❖ Anisotropies in spectra of emitted particles and methods used
 - ✧ Collectivity in Pb-Au collisions at the SPS
 - ✧ Jet suppression at the LHC
 - ✧ Collectivity in ultra-central collisions at the LHC
 - ✧ Factorization breaking – a connection with viscosity in QGP
 - ✧ Sub-leading flow modes from data and a model using the PCA
 - ✧ Correlations between different harmonics and hydrodynamics probes
- ❖ Summary

Quark-gluon and Electromagnetic plasma



Schematic view of

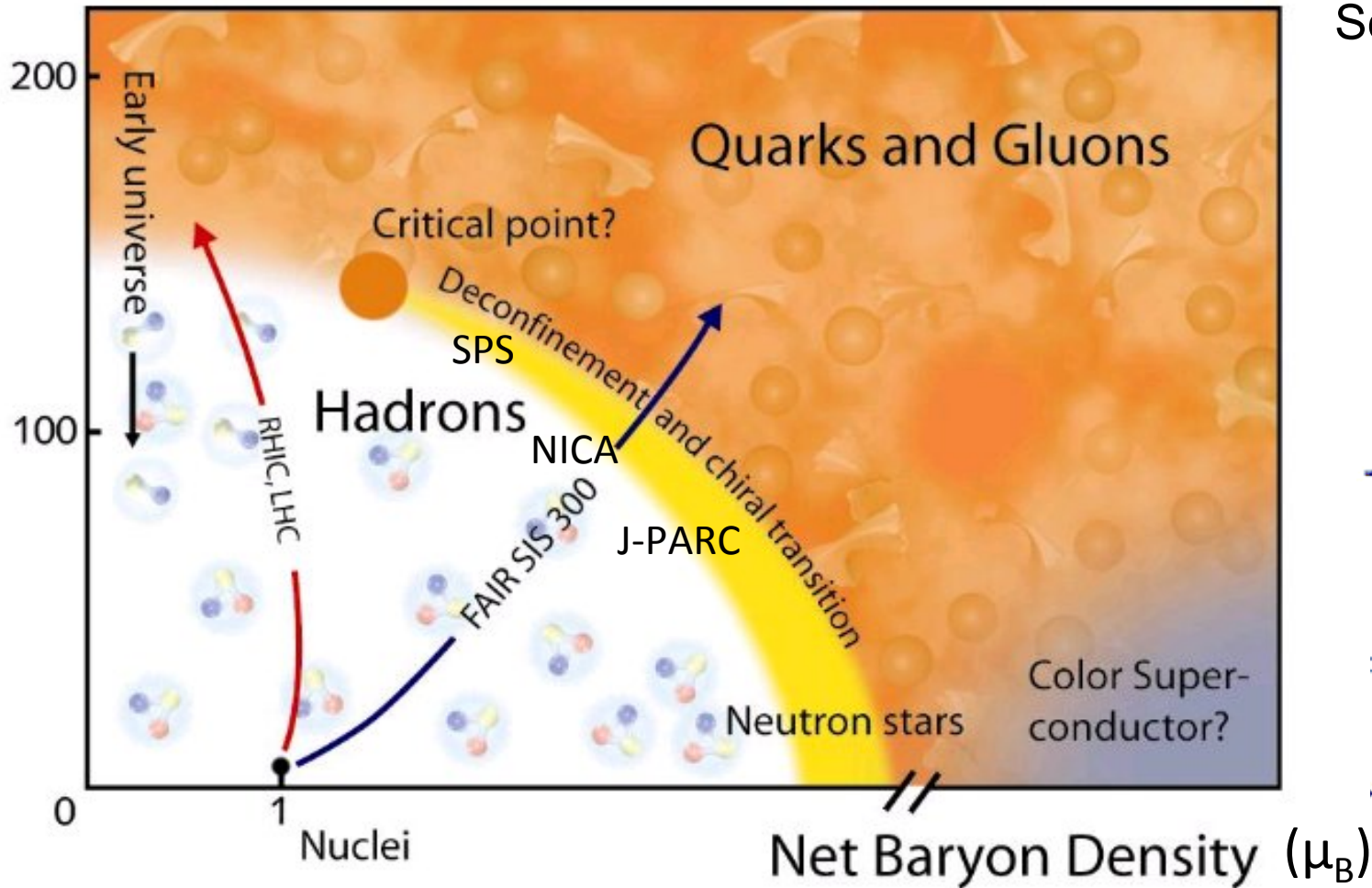
the QGP

the electromagnetic plasma

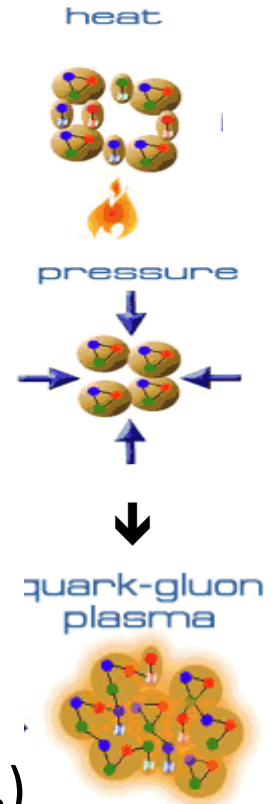
- ❖ Both are built out of the deconfined basic constituents: quarks and gluons, and electrons and ions
- ❖ Strength of the interaction (QCD vs EM) is drastically different: 1 to $1.4 \cdot 10^2$ at transfer momentum Q of 1 GeV
- ❖ Thus, there is a fast thermalization of the formed system of partons
- ❖ QGP is a strongly interacting liquid rather than the weakly interacting gas of partons

T- μ_B phase diagram of nuclear matter

Temperature T [MeV]

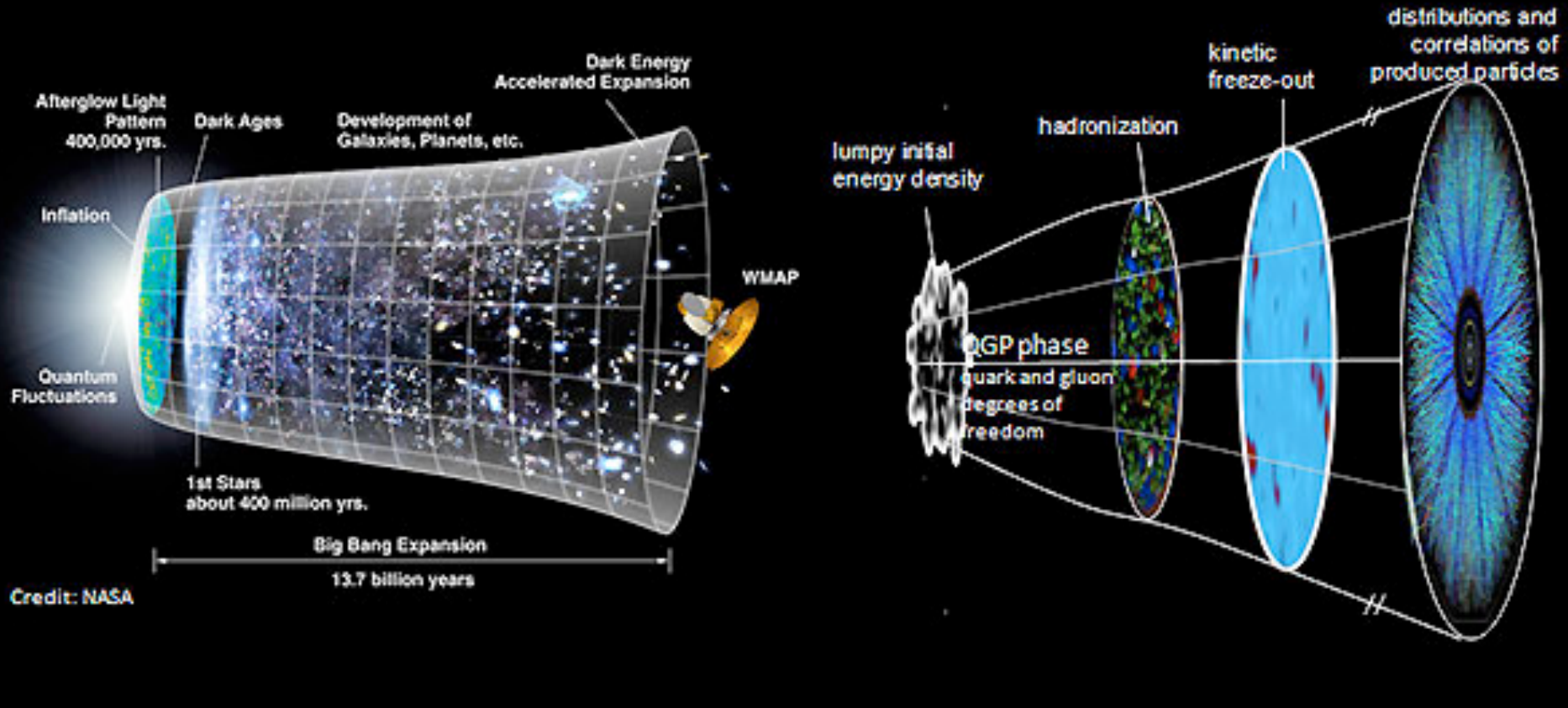


Schematic view



- ❖ QGP discovered at high T (~ 170 MeV) and low μ_B (~ 0) at Relativistic Heavy Ion Collider (RHIC) and Large Hadron Collider (LHC) – corresponds to the early Universe
- ❖ QCD phase structures (first-order phase transition, critical point) should exist in high density regime – could correspond to some astrophysical objects and some exotic states

Early Universe and relativistic collisions of nuclei



Schematic view of the Universe and the relativistic collision of nuclei

There are similarities between the early phase of the Universe (1 μ s after Big Bang) and rel. nucl. collisions: QGP phase and hadronization (confinement of partons)

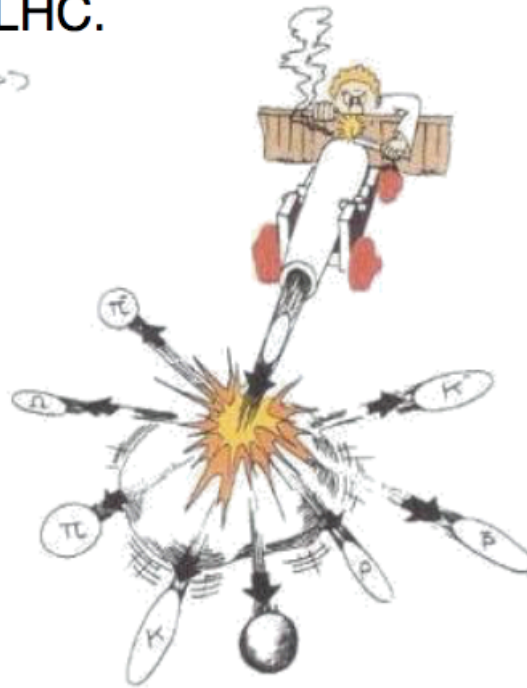
Evolution of experiments in collisions of nuclei

..from early fixed target experiments at GSI/Bevalac and SPS to collider experiments at RHIC and LHC.



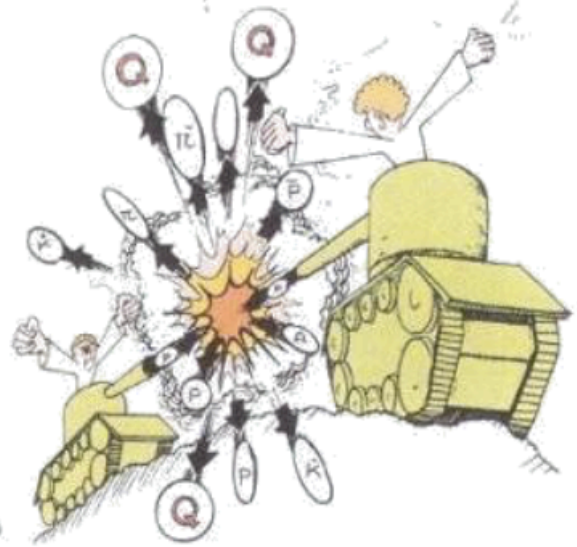
SIS

GSI Darmstadt, $\sqrt{s_{NN}} \sim 2.4$ GeV



SPS

CERN, $\sqrt{s_{NN}} \sim 6-20$ GeV



RHIC/LHC

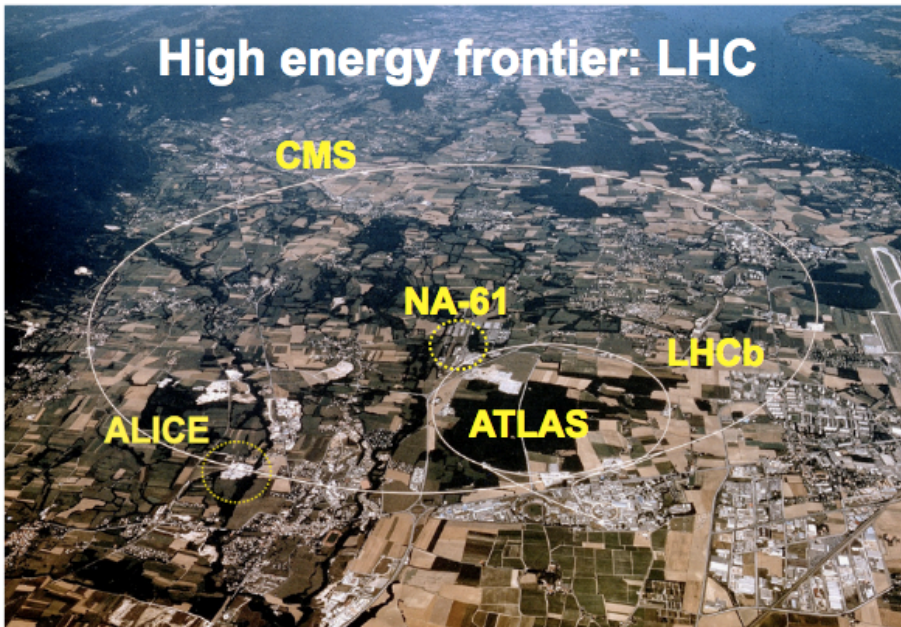
Brookhaven \rightarrow RHIC $\sqrt{s_{NN}} \sim 8-200$ GeV (BES)
 CERN \rightarrow LHC $\sqrt{s_{NN}} = 5.02$ TeV

Today there is an increasing interest in nuclear collisions at lower energies (5 – 11 GeV):
NICA (Dubna), **CBM** (GSI, Darmstadt) and **J-PARC** (Tokai)

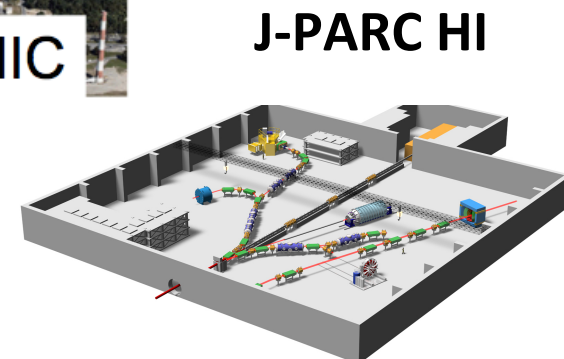
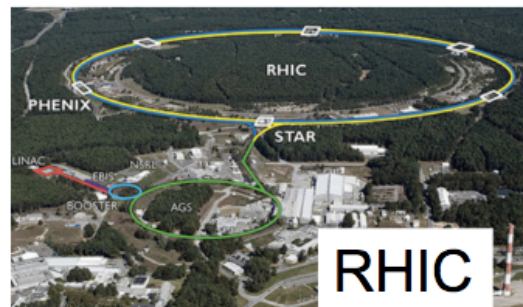
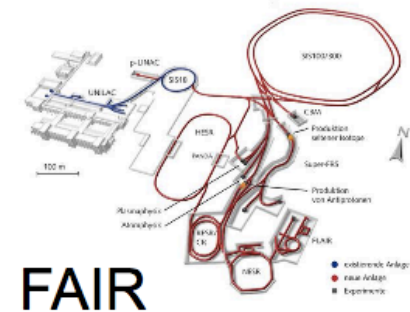
Some of existing and future experiments

Heavy-ion experiments

High energy frontier: LHC



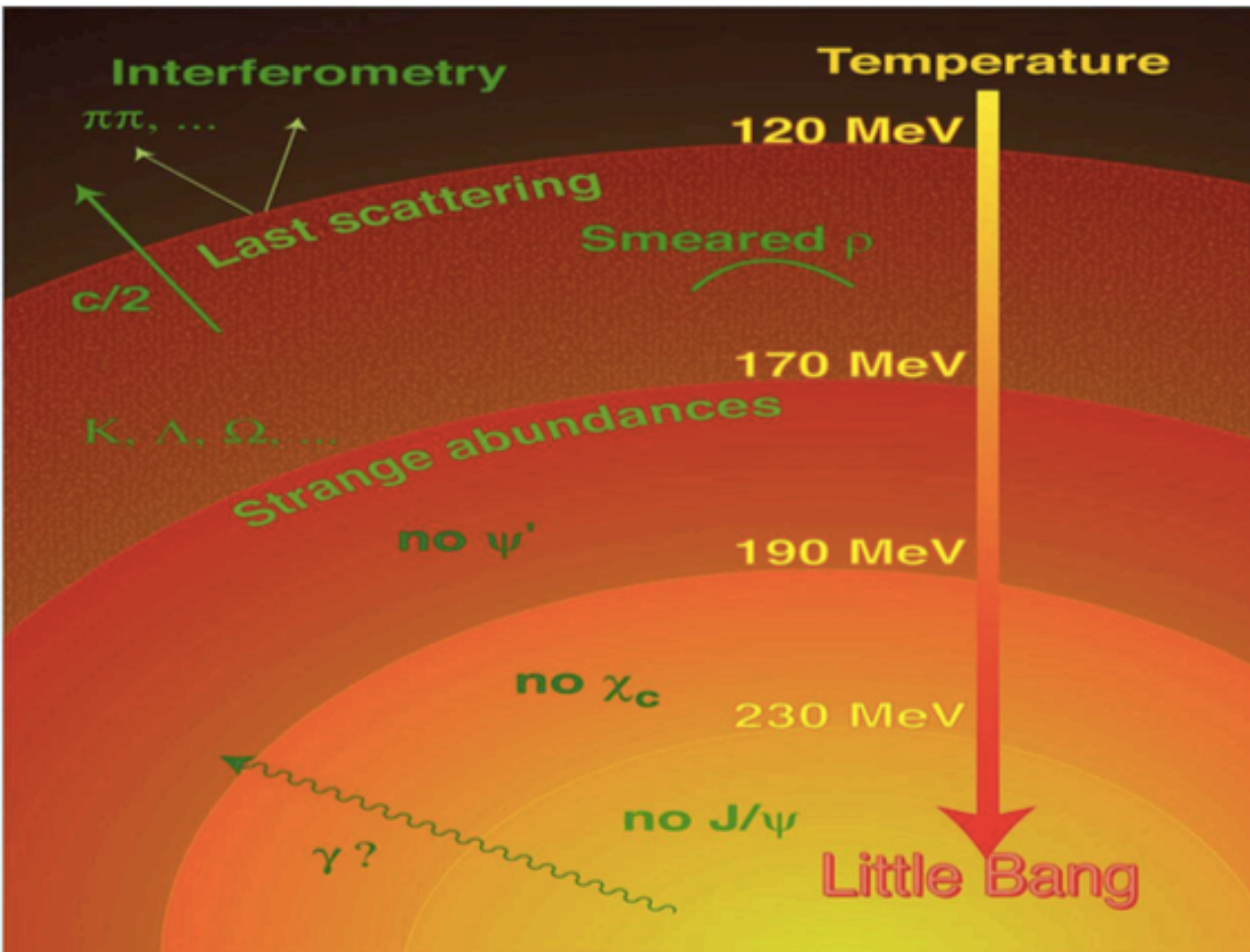
Low energy frontier: RHIC (BES), SPS
→ future facilities: FAIR (GSI), NICA



→ By now all major LHC experiments have a heavy-ion program: LHCb took Pb-Pb data for the first time in November 2015.

There are also plans of building huge colliders like FCC (CERN) and CEPC (China) which will have Heavy Ion Program too

How to investigate QGP

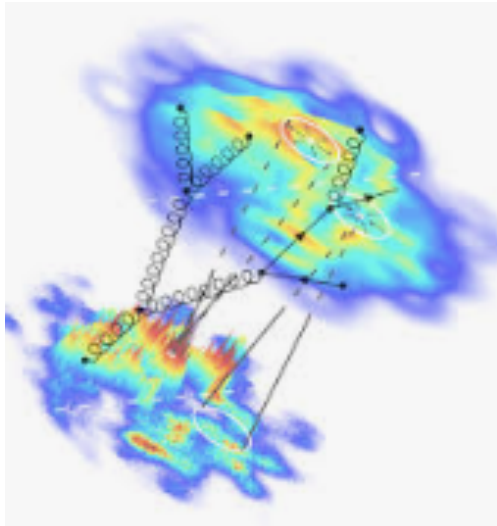
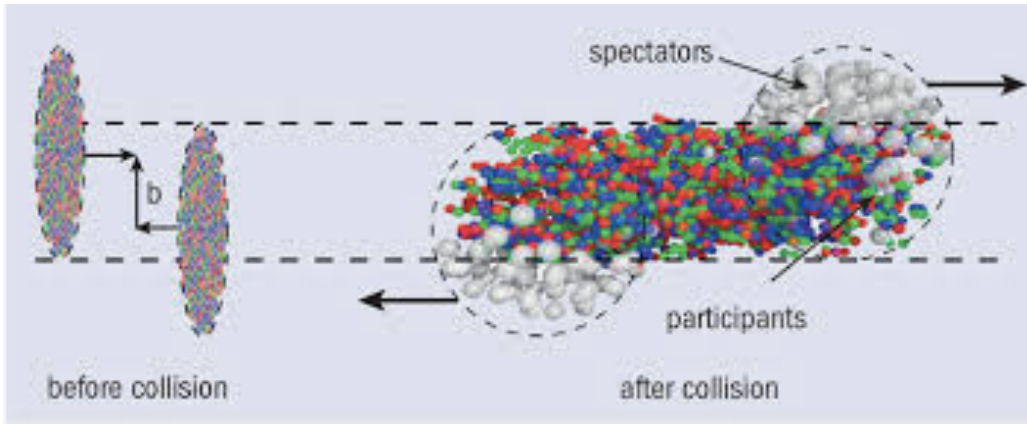


- ❖ Particle spectra
- ❖ Change of strangeness
- ❖ Particle ratios
- ❖ Particle interferometry (HBT)
- ❖ Direct photons
- ❖ Thermal leptons
- ❖ Change of particle properties in the medium
- ❖ Jet quenching
- ❖ Collective movements
- ❖ Fluctuations

Experimentalists from Serbia are mainly involved in collective movements, fluctuations and jet quenching

In cooperation with China we founded *Strong-coupling Physics International Research Laboratory*

Theoretical models to describe HI evolution and QGP



Hadronic cascade

- ❖ Ultra relativistic Quantum Molecular Dynamics (**UrQMD**)
- ❖ Quark Gluon String Model (**QGSM**)
- ❖ A Multi Phase Transport Model (**AMPT**)
- ❖ Jet AA Microscopic Transport Model (**JAM**)
- ❖ ...

Relativistic liquid

- ❖ Hydrodynamics model (**iEBE-VISHNU**)
- ❖ HYDroynamics plus JETs (**HYDJET++**)
- ❖ ...

Hybrid models

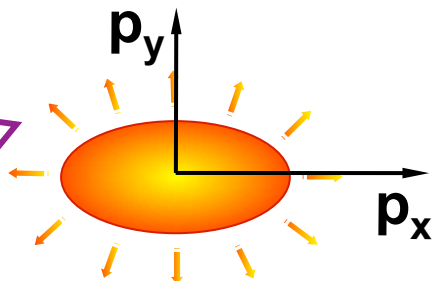
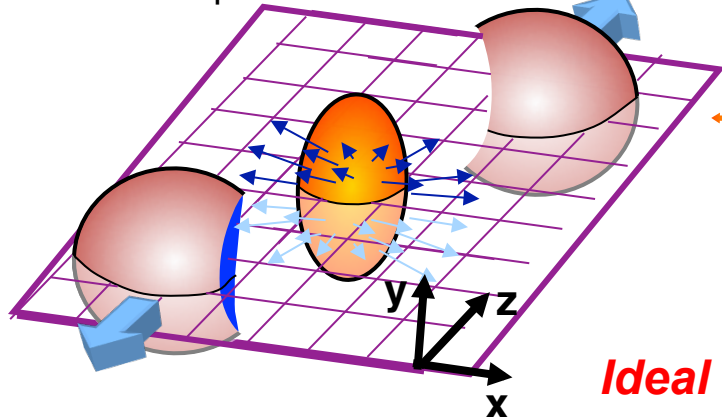
- ❖ **vHLE viscous + UrQMD**

Models are not universal. Dependence of different collision energies (range MeV to TeV)
To check different observables to make possible distinction between different models

Anisotropy harmonics v_n – methods

Event Plane (EP) method

event plane x-z



$$v_n = \langle \cos n(\phi - \Psi_n) \rangle$$

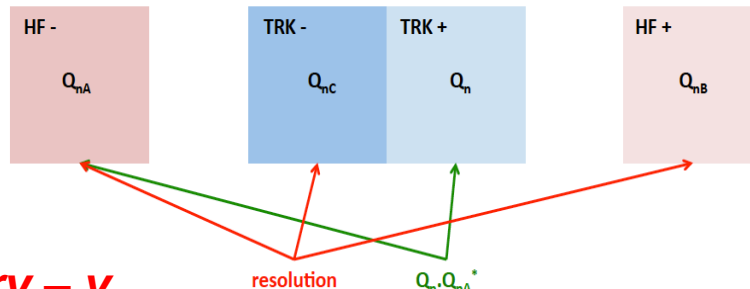
Ideal circle-like geometry – v_2

Scalar Product (SP) method

$$|\Delta\eta| > 3$$

$$v_n\{SP\} = \frac{\langle Q_n \cdot Q_{nA}^* \rangle}{\sqrt{\frac{\langle Q_{nA} \cdot Q_{nB}^* \rangle \cdot \langle Q_{nA} \cdot Q_{nC}^* \rangle}{\langle Q_{nB} \cdot Q_{nC}^* \rangle}}}$$

$$Q_n = \sum_i e^{in\phi}$$

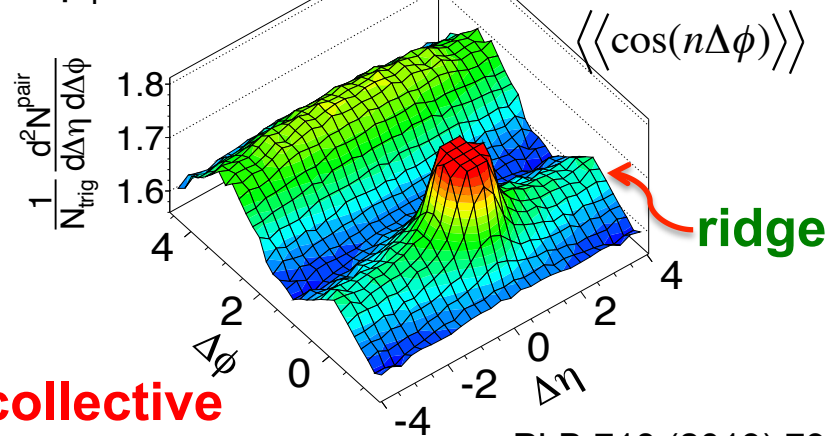


two-particle correlation method

pPb 5.02 TeV

$1 < p_T < 3$ GeV/c

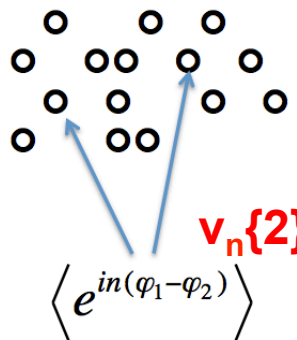
0-3% centrality
 $N > 110$



collective behavior?

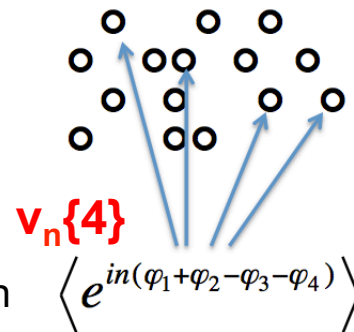
PLB 718 (2013) 795

four-particle cumulant method



Advantage wrt

2-part.corr.:
removes two-
and three-
particle non-
flow correlation



◆ v_n from even higher order cumulants:

$v_n\{6\}, v_n\{8\}, \dots$

Lee-Yang zero method

correlates all particles of interest

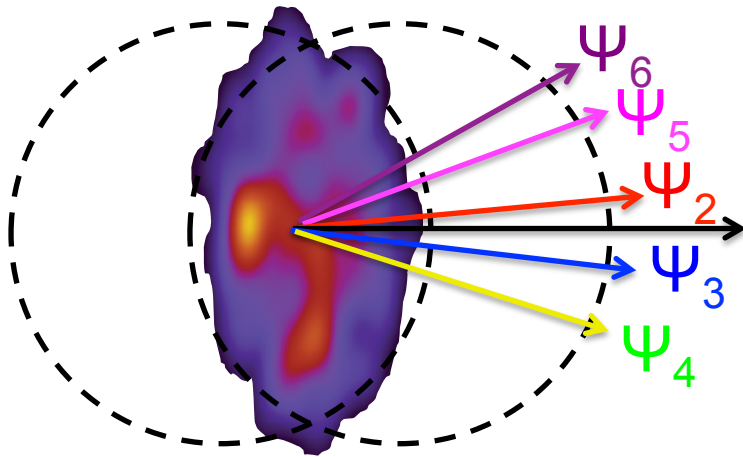
Principal Component Analysis

flow modes of higher orders

Initial state fluctuations and anisotropies

Anisotropy harmonics with order higher than 2

geometry – v_2
ISF – v_3

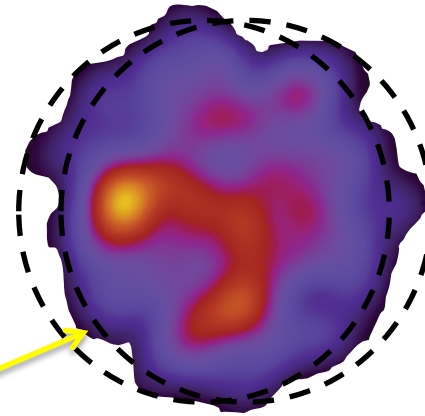


v_2, v_3, v_4, v_5 and v_6
using multiple methods

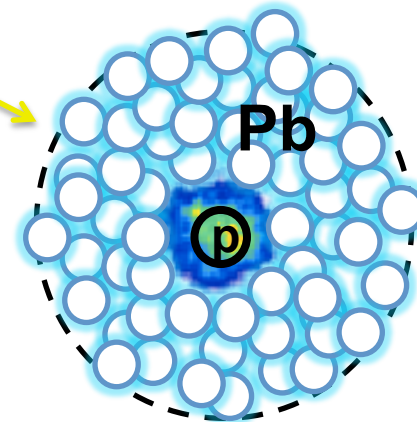
Simple, circle-like geometry does not describe the formed system precisely enough

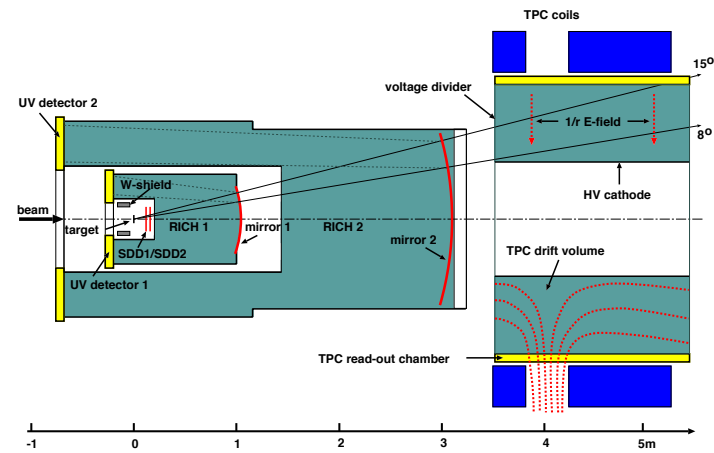
initial-state fluctuations dominates

Ultra-central collisions

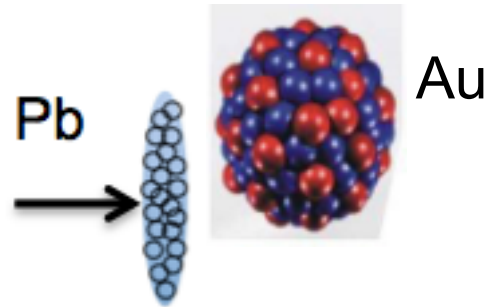


Asymmetric (pPb) high-multiplicity collisions





Anisotropies from the CERES/NA45 at the SPS in PbAu collisions



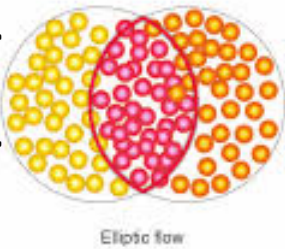
Fixed target experiment

Elliptic flow in PbAu at the top SPS energy

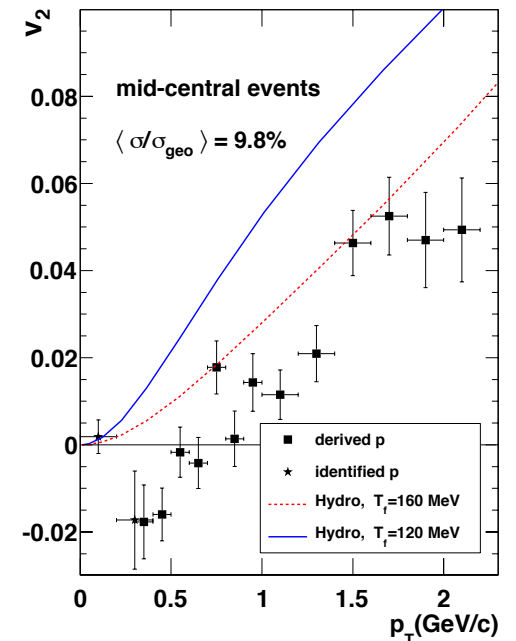
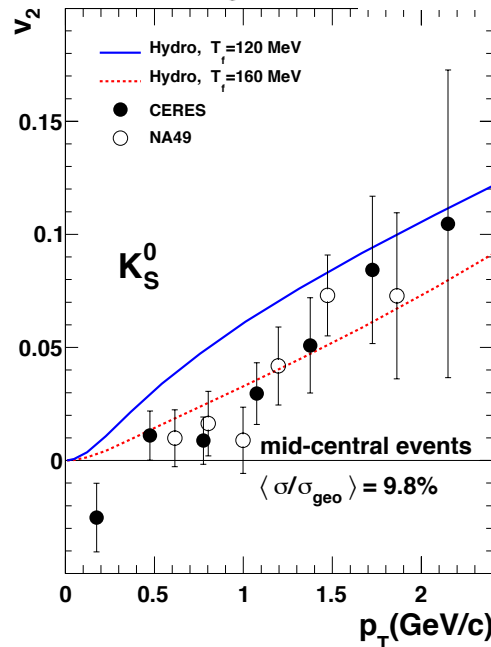
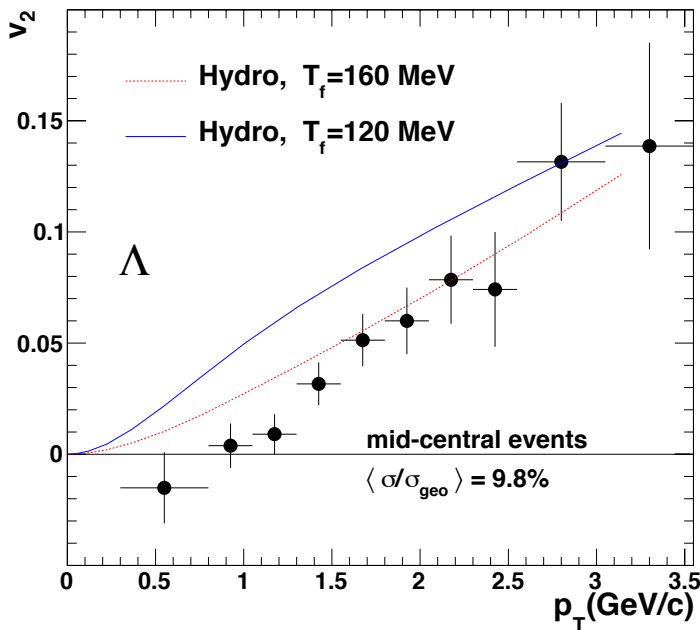
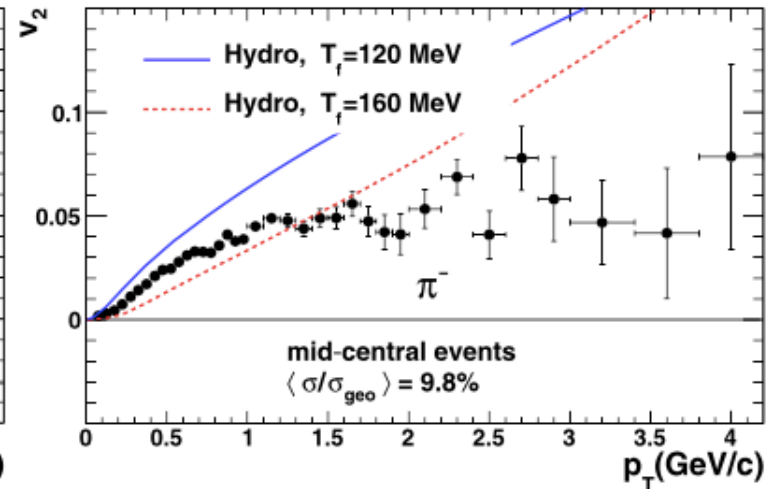
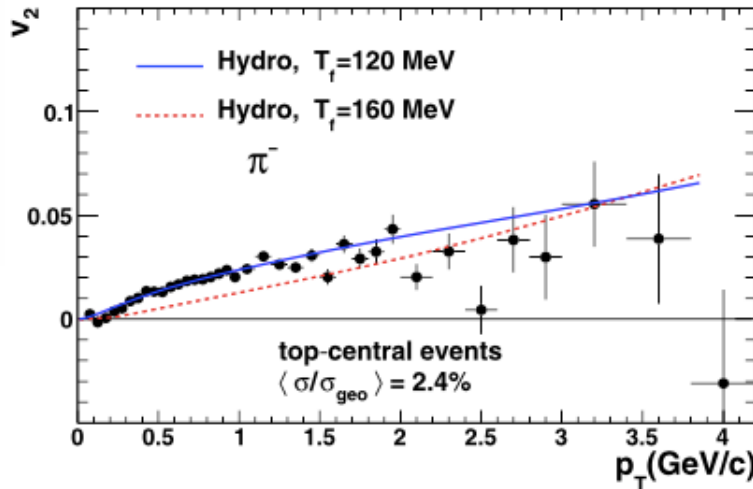
≈30M PbAu collisions collected during 2000 data taking period

$$\sigma/\sigma_{\text{geo}} = \langle 5.5\% \rangle \quad \sqrt{s_{NN}} = 17.3 \text{ A GeV}$$

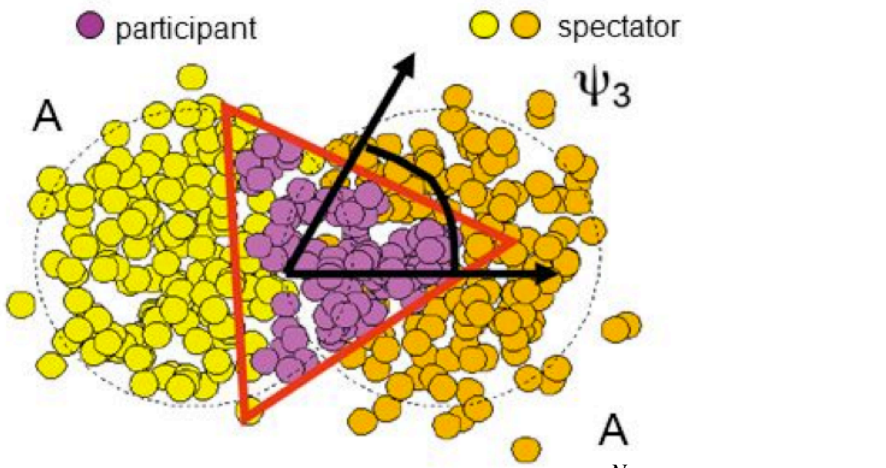
Nucl.Phys.A894 (2012) 41



EP method is used



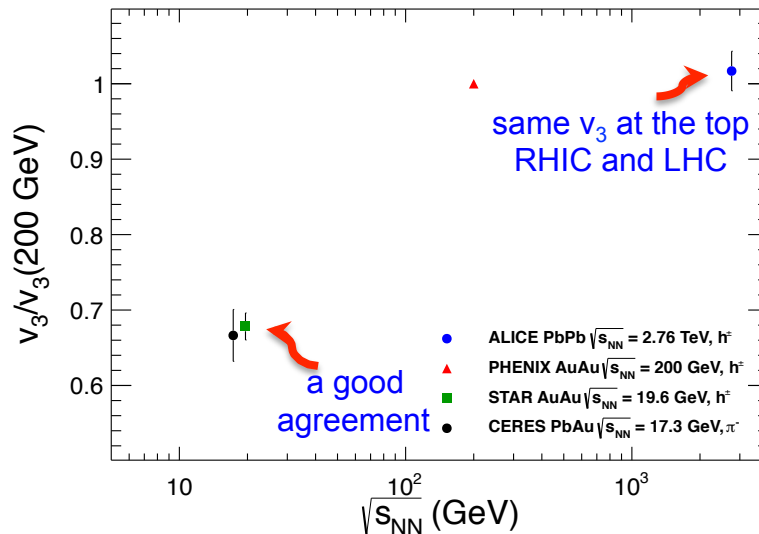
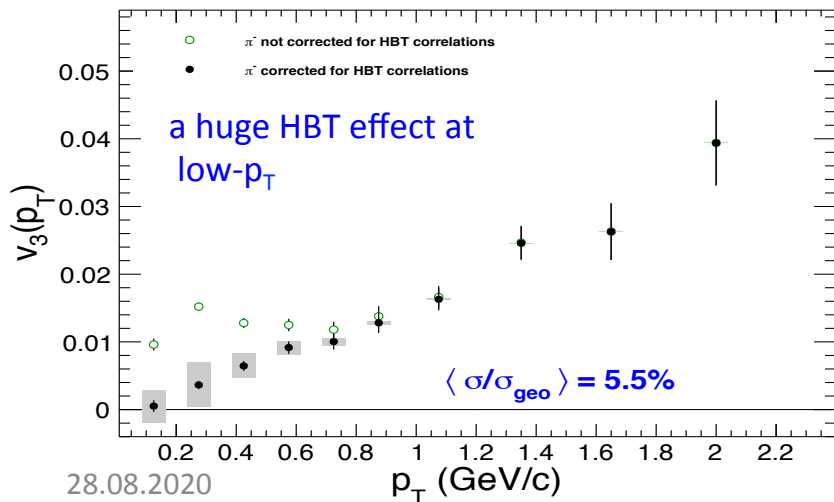
Triangular flow in PbAu at the top SPS energy



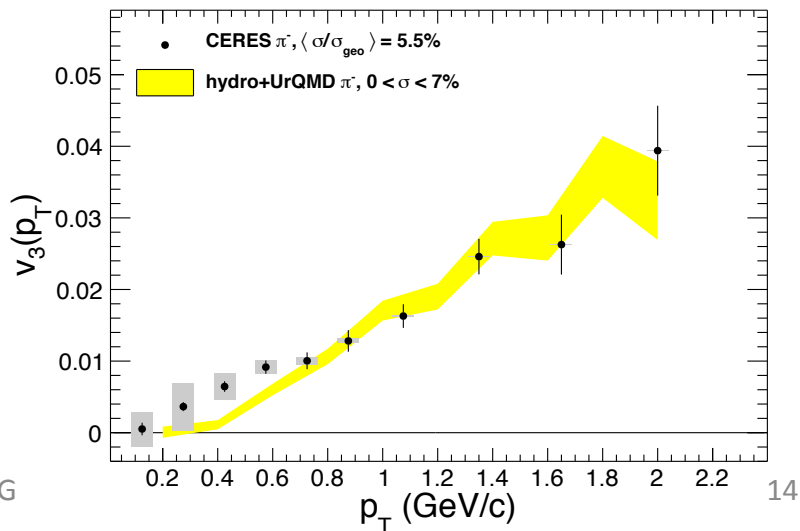
EP method
is used

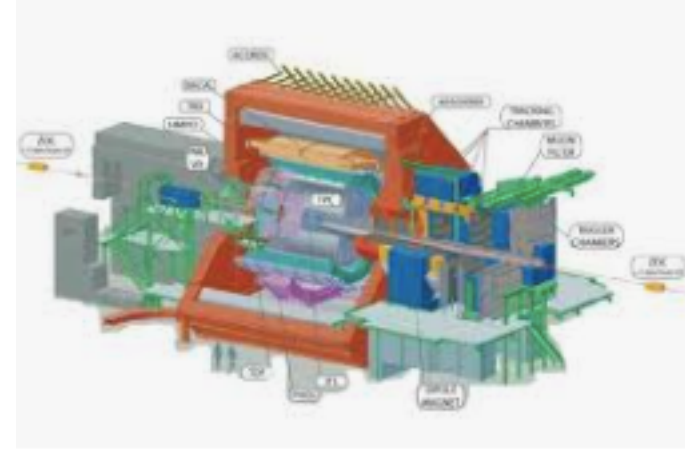
$$\Psi_3 = \frac{1}{3} \arctan \frac{\sum_{i=1}^{N_{\text{track}}} w_i(p_{Ti}) \sin(3\phi_i)}{\sum_{i=1}^{N_{\text{track}}} w_i(p_{Ti}) \cos(3\phi_i)}$$

Nucl.Phys.A957 (2017) 99

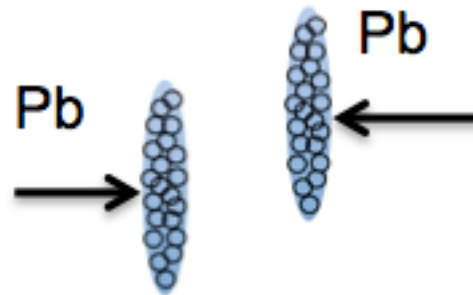


- ❖ v_2 reflects the initial anisotropy and thus **depends strongly on centrality**
- ❖ v_3 comes from the ISF and **weakly depends on centrality**





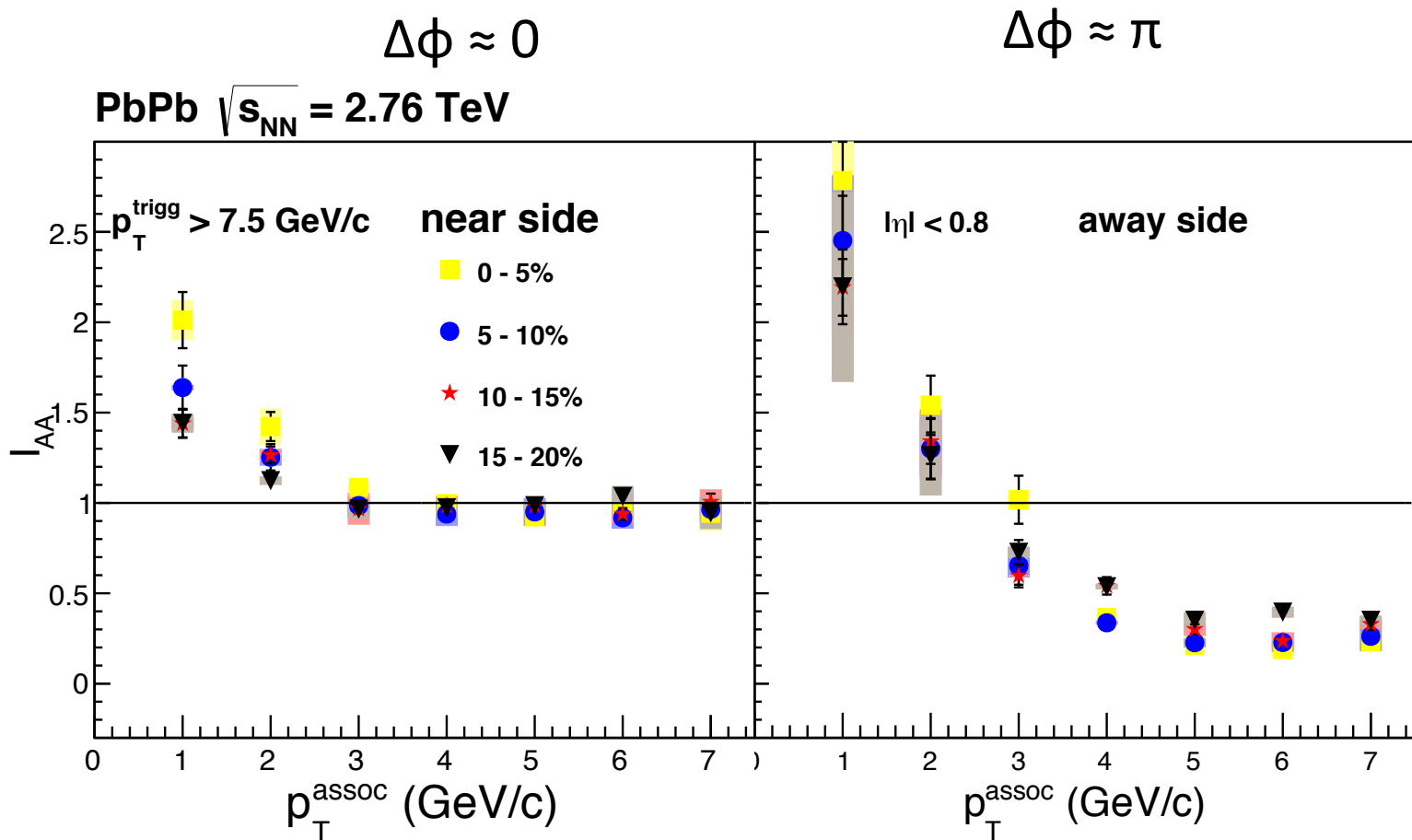
Jets from the ALICE at the LHC in PbPb collisions

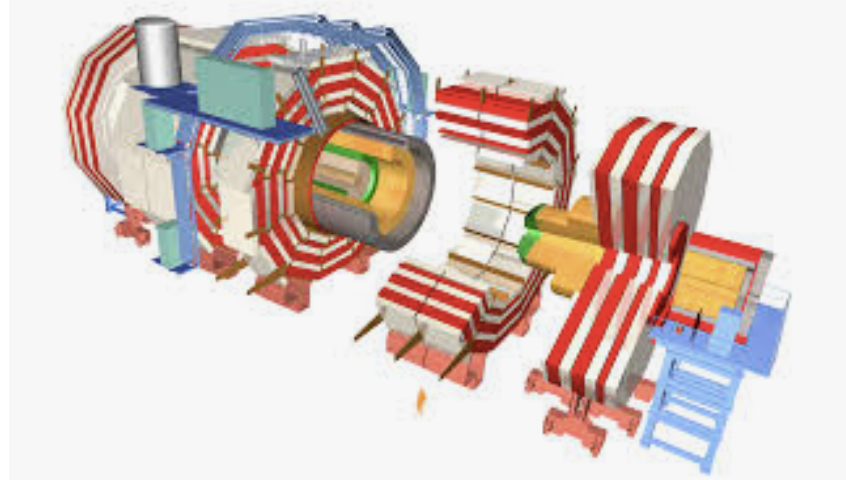


Collider experiment

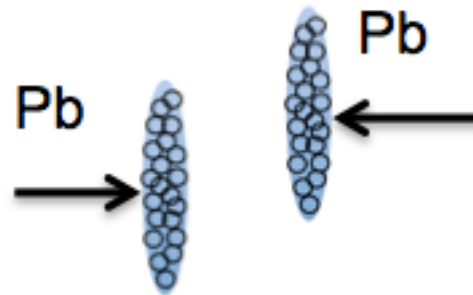
Jet quenching in QGP from PbPb collisions

- ❖ I_{AA} defined as a ratio of jet yields in PbPb and pp collisions at a given p_T
- ❖ Significant enhancement for all centralities at low- p_T on both sides
- ❖ Strong suppression at high p_T on the away side (a long path travel through QGP)
- ❖ On the near side there is no suppression (a short path travel through QGP)





Anisotropies from the CMS at the LHC



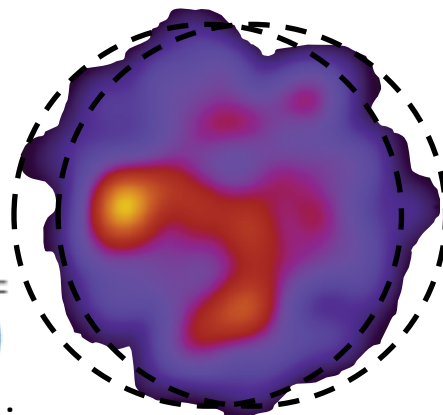
Collider experiment

v_n at 2.76 TeV ultracentral PbPb collisions

- ❖ CMS is able to extract ultracentral (0-0.2% centrality) PbPb collisions
- ❖ v_2 strongly depends on centrality even for very central collisions, while v_n ($n=3, \dots$) weakly depends on centrality

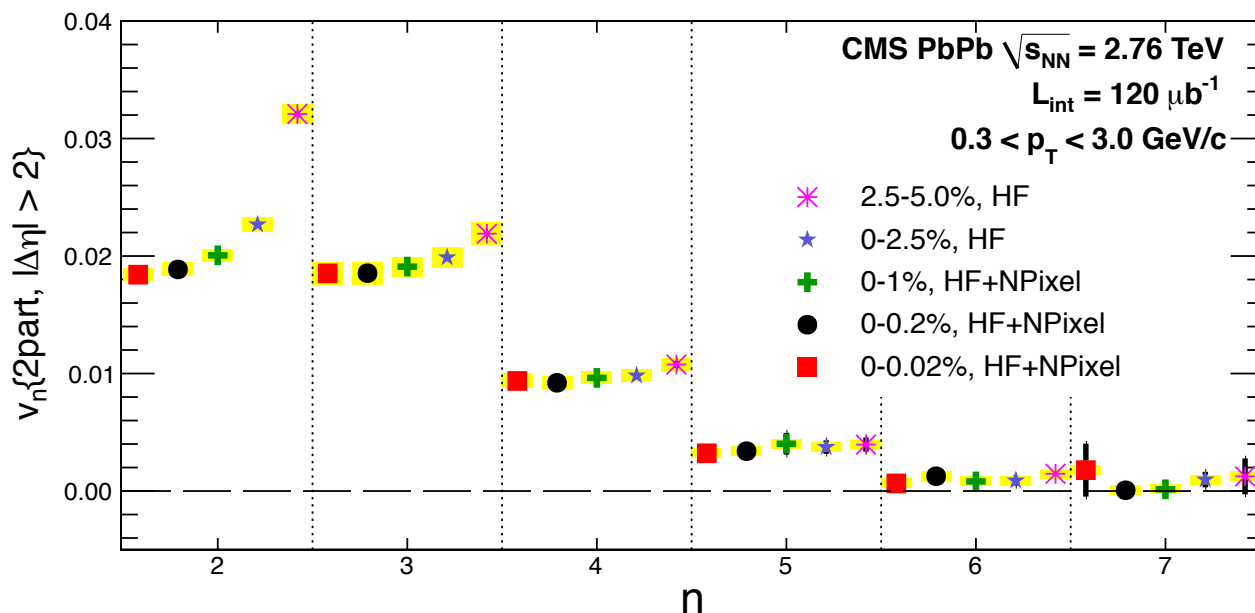
$$V_{n\Delta} = \langle\langle \cos(n\Delta\phi) \rangle\rangle_S - \langle\langle \cos(n\Delta\phi) \rangle\rangle_B$$

$$V_{n\Delta} = v_n(p_T^{\text{trig}}) \times v_n(p_T^{\text{assoc}}) \quad v_n(p_T) = \frac{V_{n\Delta}(p_T, p_T^{\text{ref}})}{\sqrt{V_{n\Delta}(p_T^{\text{ref}}, p_T^{\text{ref}})}}$$



In UCC, anisotropy comes entirely from the initial-state fluctuations

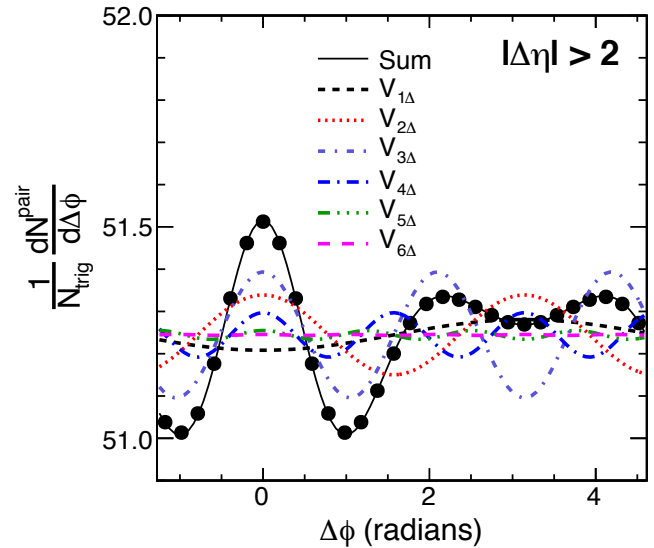
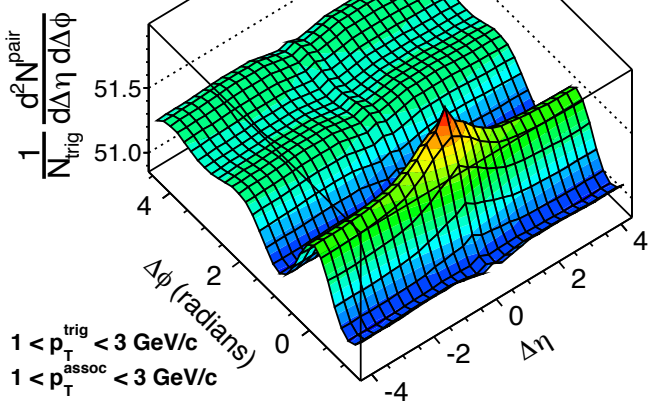
Method of
2-particle
2-dimensional
(in $\Delta\eta$ and in
 $\Delta\phi$)
correlations



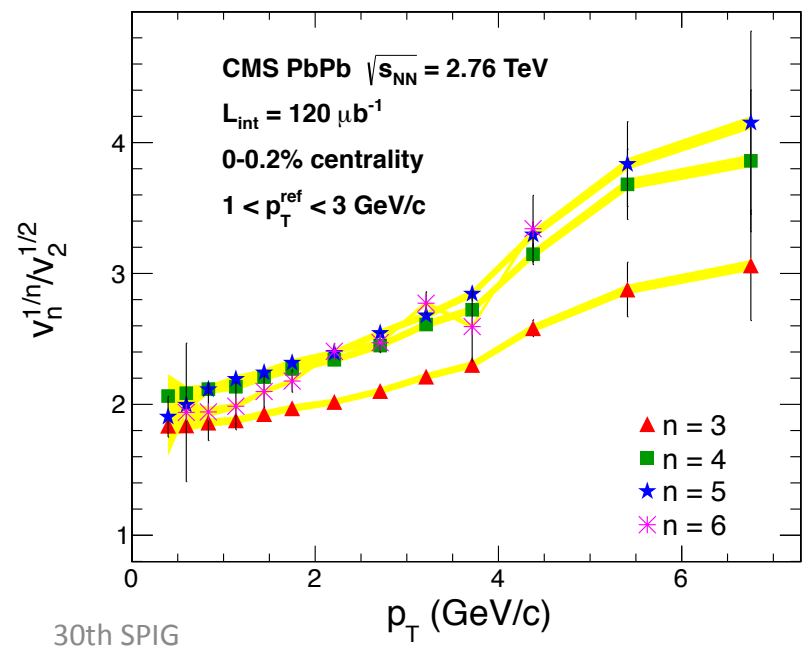
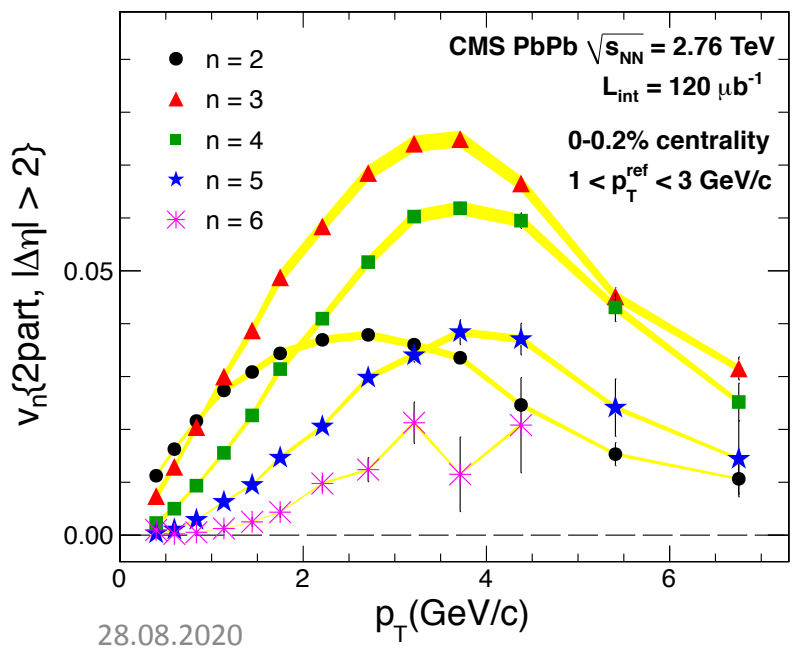
CMS
JHEP 1402 (2014) 088

v_n at 2.76 TeV ultracentral PbPb collisions

CMS PbPb $\sqrt{s_{NN}} = 2.76$ TeV
 $L_{int} = 120 \mu b^{-1}$
 0-0.2% centrality



- ❖ possibility to extract high orders v_n harmonics
- ❖ v_3 is dominant anisotropy for ultracentral collisions
- ❖ In ideal hydro $v_n^{1/n} / v_2^{1/2}$ should be independent on p_T



CMS
 JHEP 1402 (2014) 088

Initial-state inhomogeneity – factorization breaking

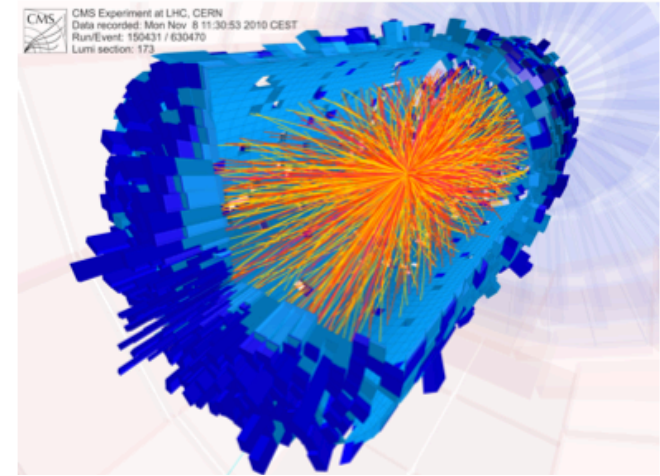
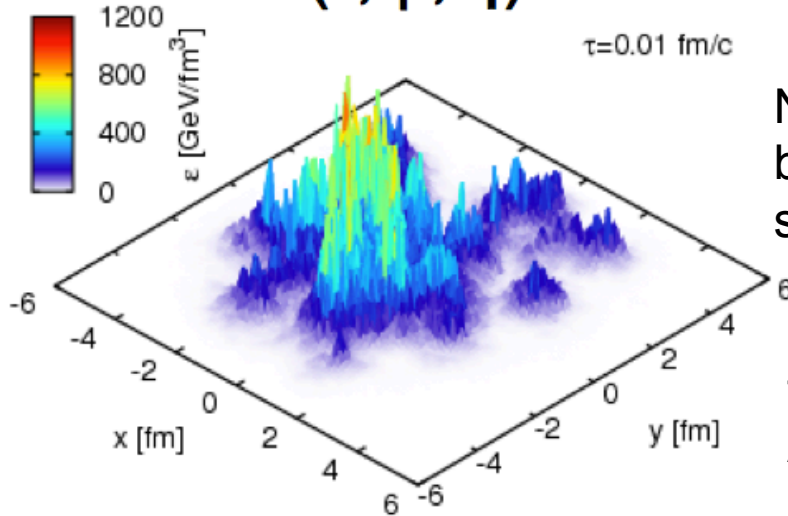
Initial state

$$\varepsilon(r, \varphi, \eta)$$

EbE hydro.

Final state

$$f(p_T, \varphi, \eta)$$

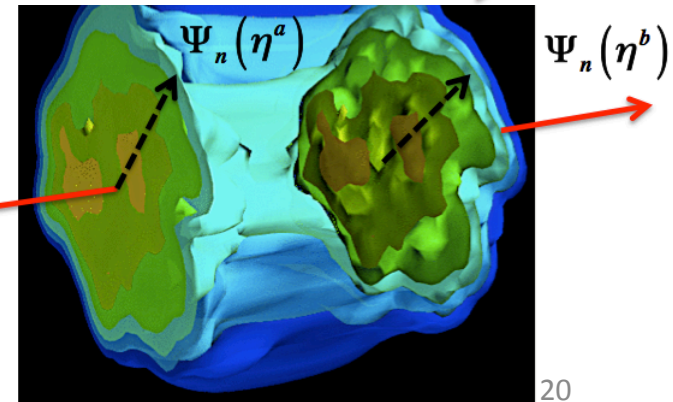


fluctuations $\Delta\varepsilon(r, \phi, \eta)$

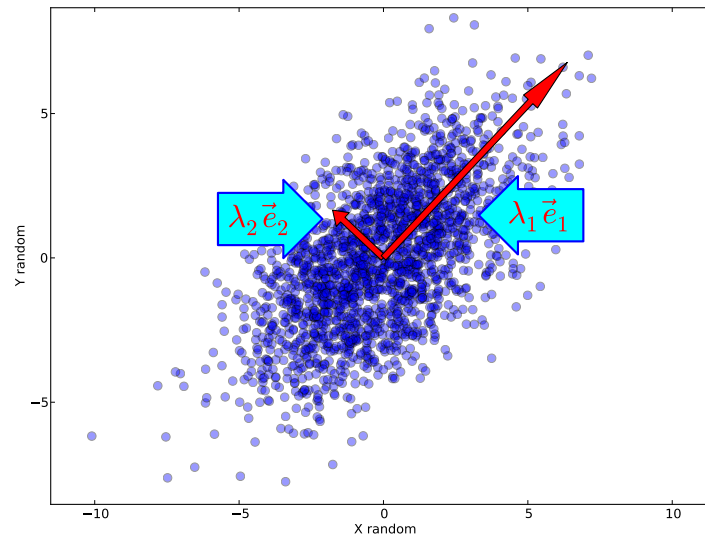
overlap zone in x-y

$$f(p_T, \phi, \eta) \sim 1 + 2 \sum_{n=1}^{\infty} v_n(p_T, \eta) \cos[n(\phi - \Psi_n(p_T, \eta))]$$

- Local hotspots perturb the EP of a smooth medium, so $\Psi_n(p_T)$ contains information about initial-state fluctuations Phys.Rev.C **92** (2015) 034911
- Within hydrodynamics, initial-state fluctuations could appear as (sub-leading) flows Phys.Rev.C **96** (2017) 064902
- Yesterday, Damir presented in details the dissipation effects in the QGP
- Possibility to extract QGP transport properties

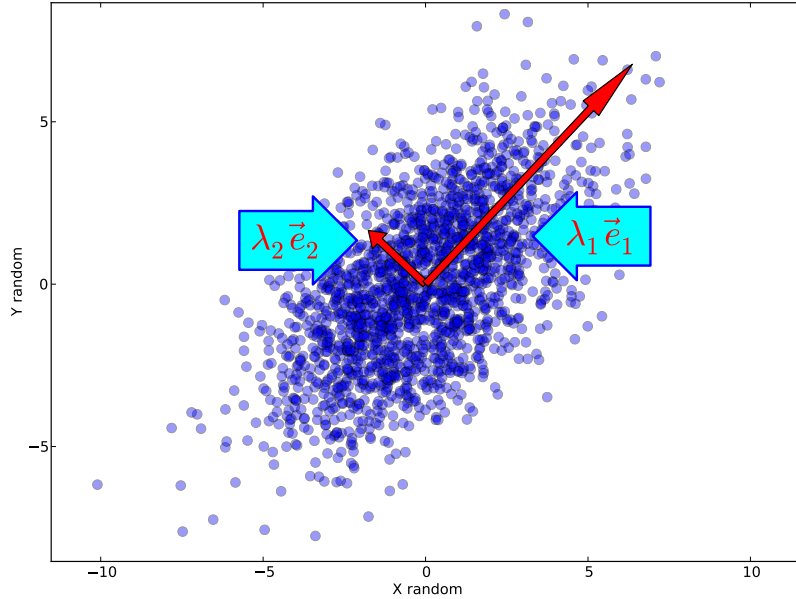


Leading and sub-leading flow from Principal Component Analysis



Principal Component Analysis (PCA) method

A simple 2D example



- ❖ Random 2D Gauss distribution
 $\vec{X}_n = (x_1, x_2, \dots, x_n)$ $\vec{Y}_n = (y_1, y_2, \dots, y_n)$
- ❖ a matrix: $\Sigma = \begin{bmatrix} \text{var}(X) & \text{cov}(X, Y) \\ \text{cov}(X, Y) & \text{var}(Y) \end{bmatrix}$
- ❖ eigenvectors e_i and eigenvalues λ_i by diagonalization Σ : $[e]^T \Sigma [e] = \text{diag}(\lambda_1, \lambda_2)$
- ❖ **First (second) Principal Component:** eigenvector e_1 (e_2) points to maximum variance of data cloud. Its magnitude is $\sqrt{\lambda_1} e_1$ ($\sqrt{\lambda_2} e_2$)

$$V_{n\Delta} = \langle\langle \cos(n\Delta\phi) \rangle\rangle_S - \langle\langle \cos(n\Delta\phi) \rangle\rangle_B$$

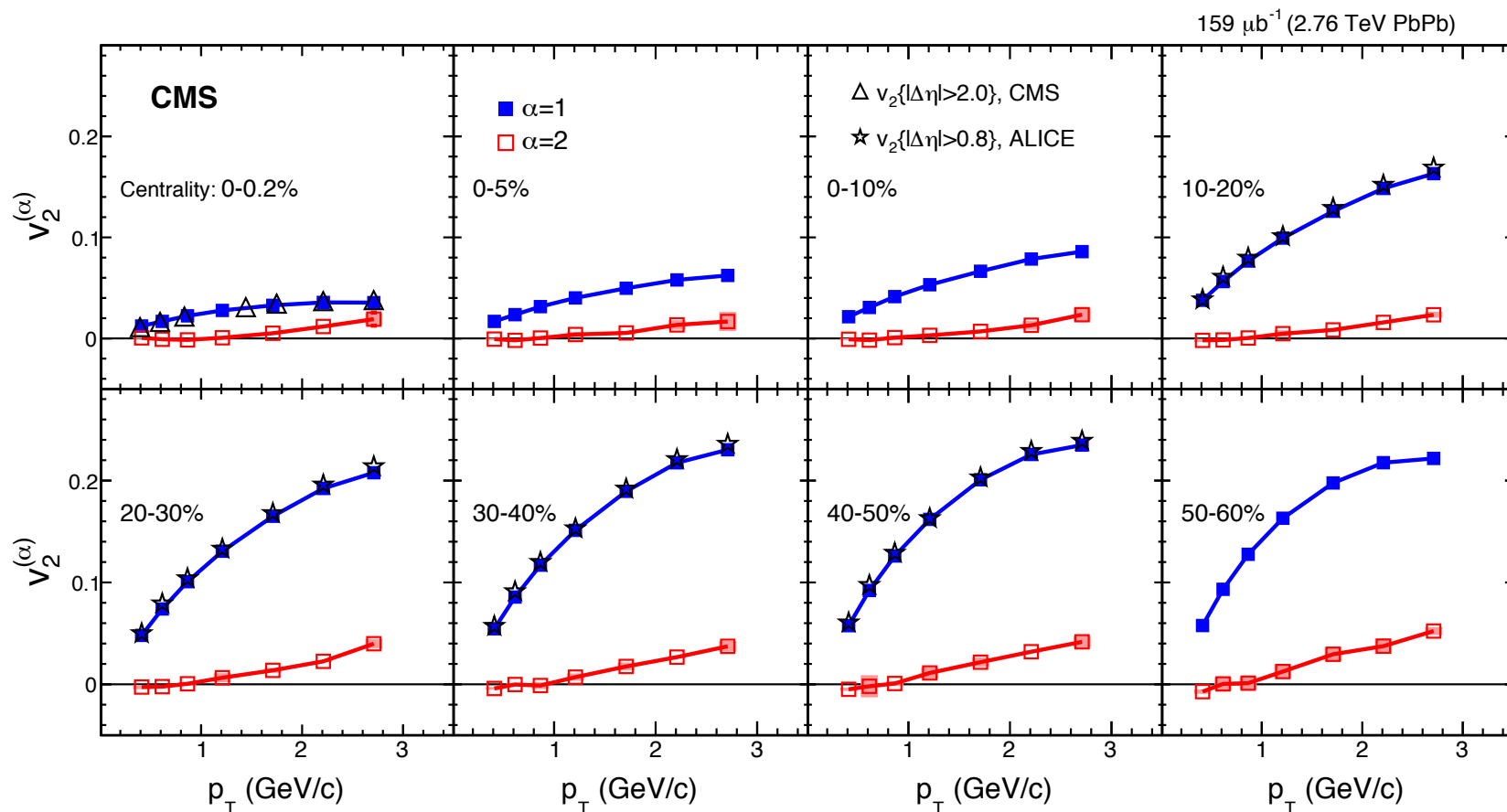
are calculated for pairs with $|\Delta n| > 2$

$$\begin{pmatrix} e^{(1)} & e^{(2)} & \dots & e^{(7)} \end{pmatrix} \begin{bmatrix} V_{n\Delta}(p_1, p_1) & V_{n\Delta}(p_2, p_1) & V_{n\Delta}(p_3, p_1) & \dots & \dots & \dots & \dots \\ V_{n\Delta}(p_1, p_2) & V_{n\Delta}(p_2, p_2) & V_{n\Delta}(p_3, p_2) & \dots & \dots & \dots & \dots \\ V_{n\Delta}(p_1, p_3) & V_{n\Delta}(p_2, p_3) & V_{n\Delta}(p_3, p_3) & \dots & \dots & \dots & \dots \\ \vdots & \vdots & \vdots & \dots & \dots & \dots & \vdots \\ \vdots & \vdots & \vdots & \dots & \dots & \dots & \vdots \\ \vdots & \vdots & \vdots & \dots & \dots & \dots & V_{n\Delta}(p_7, p_7) \end{bmatrix} \begin{pmatrix} e^{(1)} \\ e^{(2)} \\ \vdots \\ \vdots \\ \vdots \\ \vdots \\ e^{(7)} \end{pmatrix} = \text{diag} \left(\lambda^{(1)} \quad \lambda^{(2)} \quad \dots \quad \lambda^{(7)} \right)$$

$$V_n^{(\alpha)}(p_i) = \sqrt{\lambda^{(\alpha)}} e^{(\alpha)}(p_i)$$

$$v_n^{(\alpha)}(p) = \frac{V_n^{(\alpha)}(p)}{\langle M(p) \rangle}$$

Results – elliptic flows in PbPb collisions



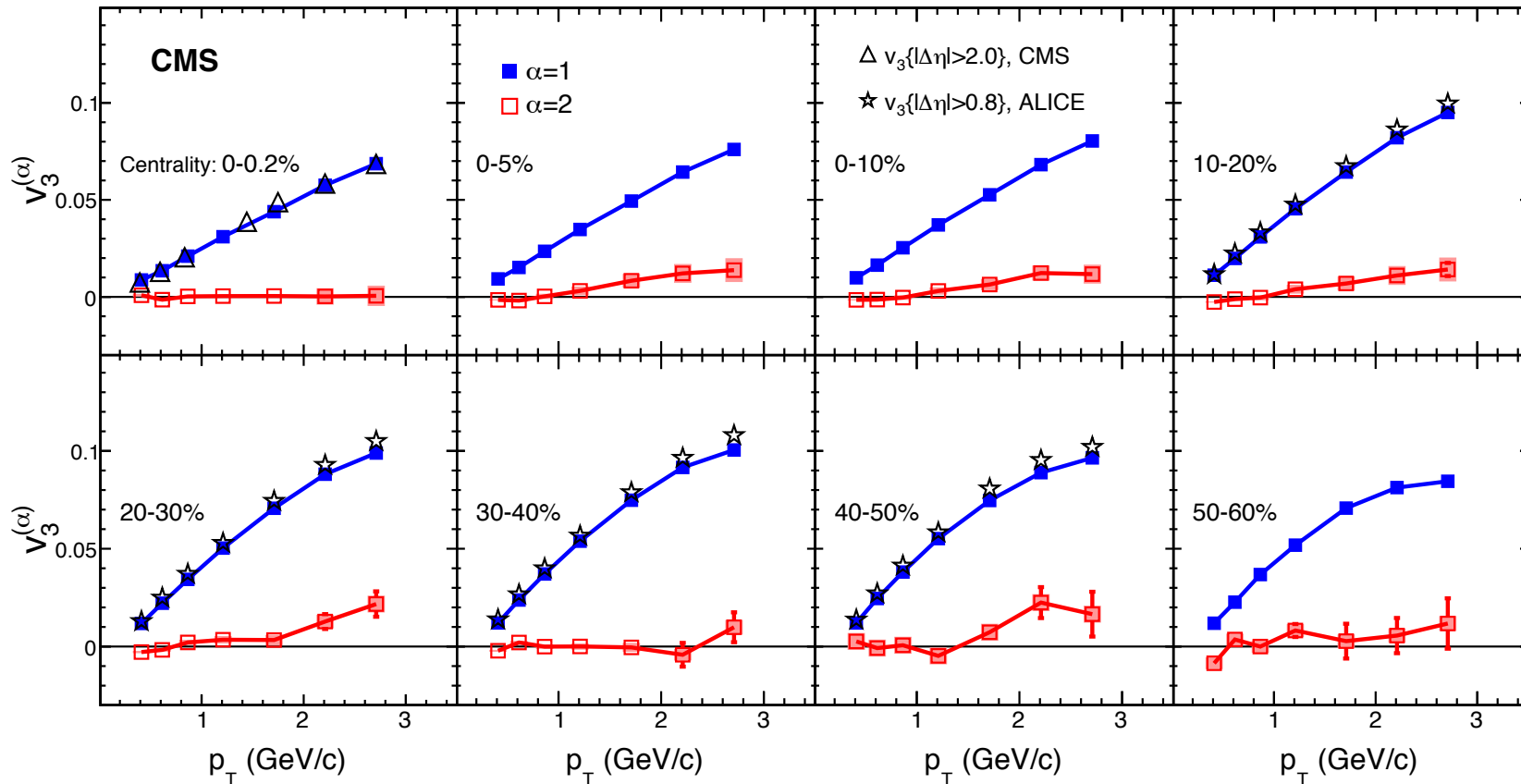
Phys. Rev. C 96 (2017) 064902

- ❖ The leading flow mode, $\alpha=1$, essentially equal to the v_2 measured by ALICE and CMS using two-particle correlations
- ❖ The sub-leading flow mode, $\alpha=2$, is compatible with zero at small p_T and then slowly increases with an increase of p_T
- ❖ It increases also with centrality
- ❖ Similar behavior wrt the r_2 results (Phys. Rev. C **92** (2015) 034911)

Results – triangular flows in PbPb collisions

159 μb^{-1} (2.76 TeV PbPb)

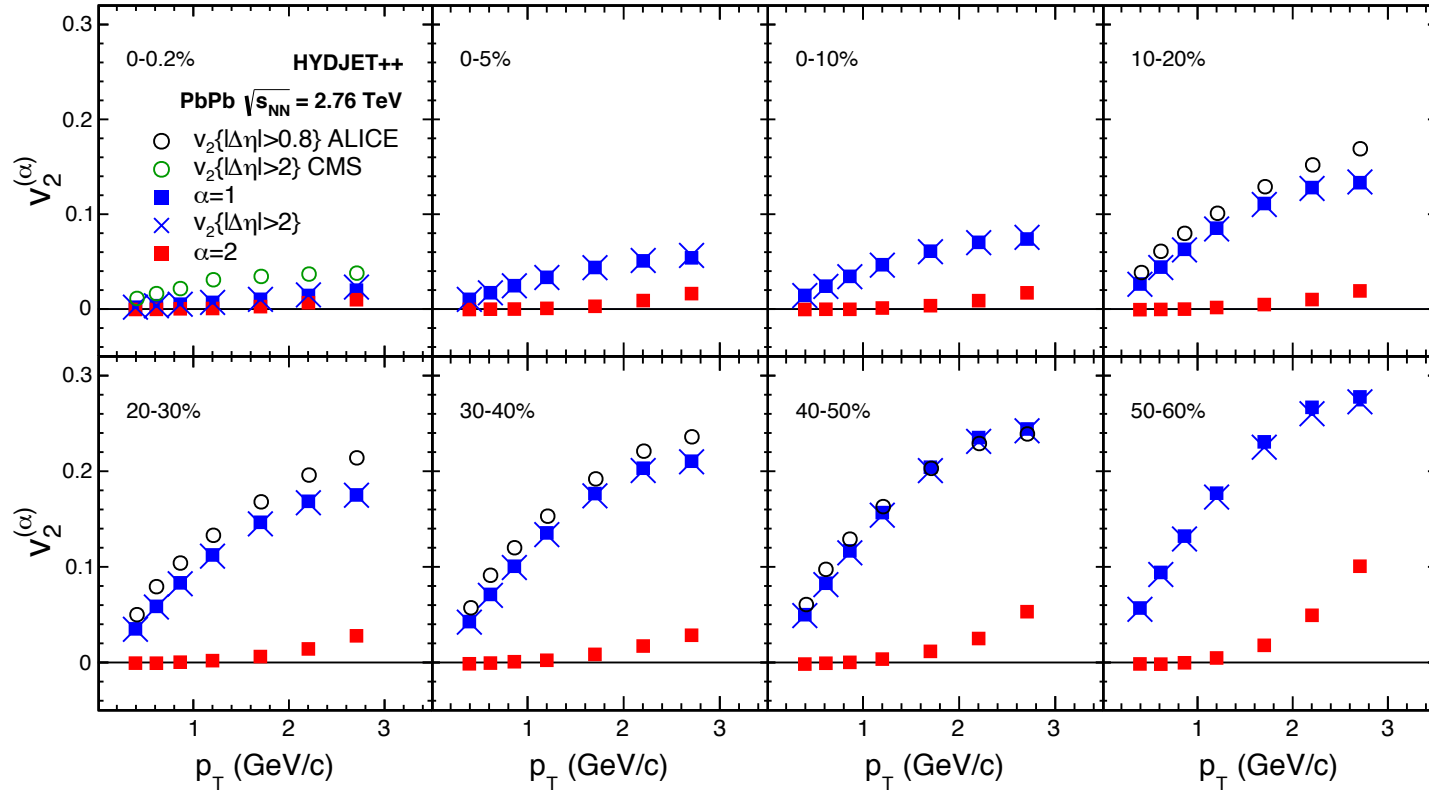
Phys. Rev. C 96 (2017) 064902



- ❖ Again, the leading flow mode, $\alpha=1$, essentially equal to the v_3 measured by ALICE and CMS using two-particle correlations
- ❖ The sub-leading flow mode, $\alpha=2$, is equal or very close to zero
- ❖ Similar centrality dependence to that observed for r_3 (Phys. Rev C 92 (2015) 034911)

Elliptic flows in HYDJET++ PbPb collisions

Data generated under
'flow'+quenched jet' switch

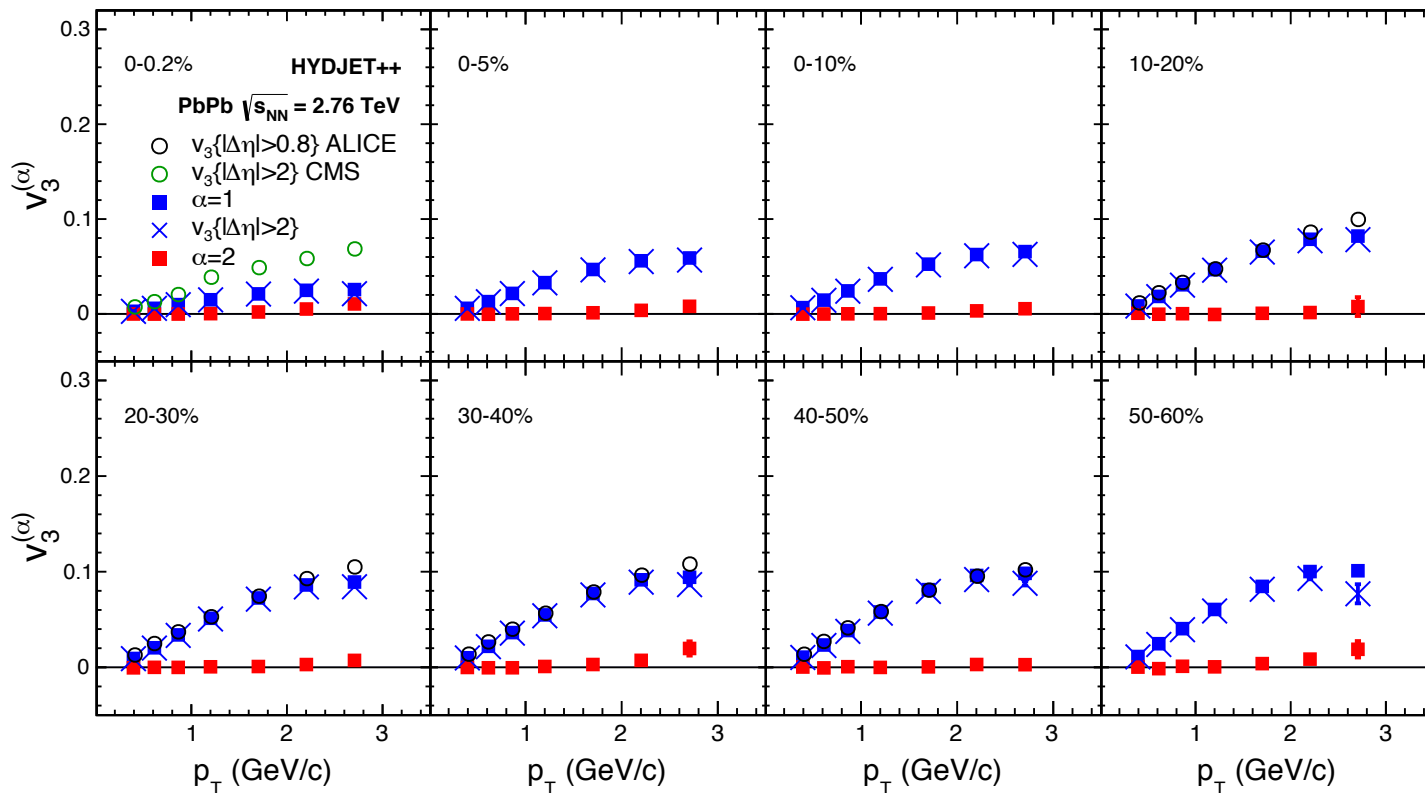


- ❖ The HYDJET++ leading flow mode, $\alpha=1$, essentially equal to the v_2 extracted from two-particle correlations. There is a rather good agreement with the v_2 experimentally measured by ALICE and CMS
- ❖ The sub-leading flow mode, $\alpha=2$, is seen for all centralities in HYDJET++ PbPb collisions generated at 2.76 TeV
- ❖ Similar behavior wrt the r_2 results (Phys. Rev. C **92** (2015) 034911)

Chin.Phys. C (2017) 074001

Triangular flows in HYDJET++ PbPb collisions

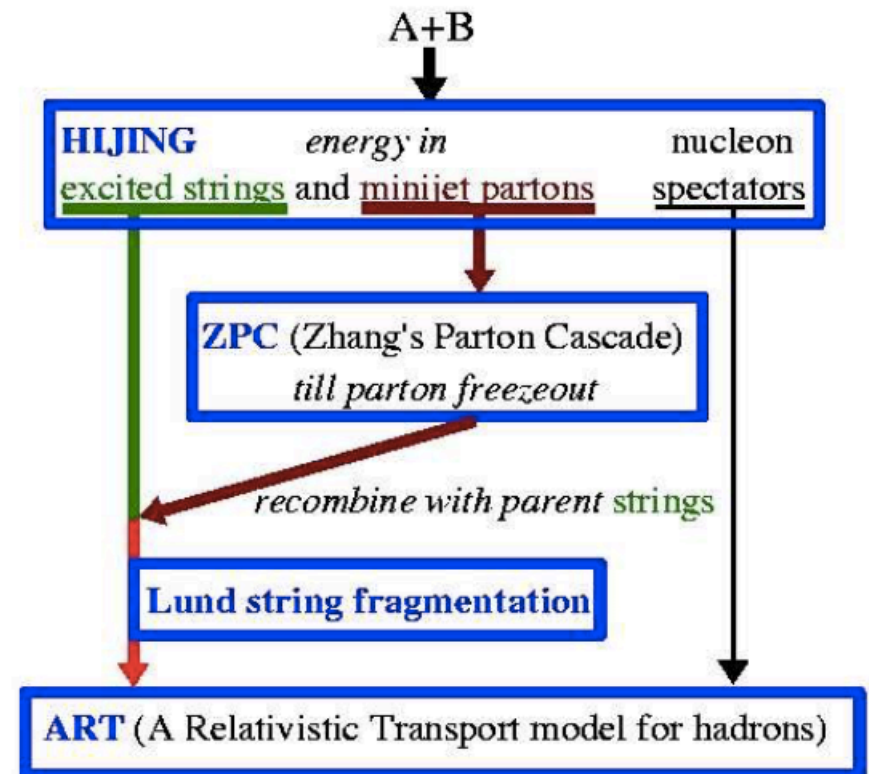
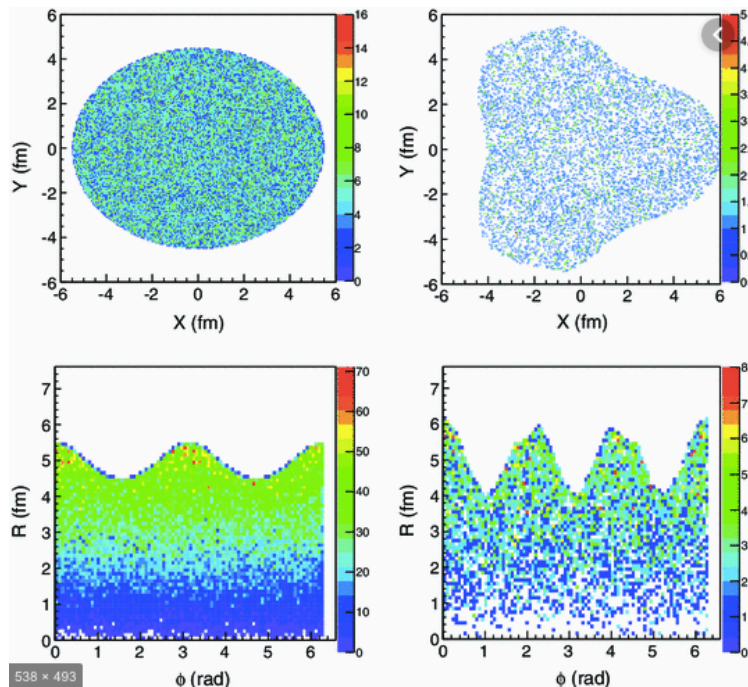
Data generated under
'flow'+quenched jet' switch



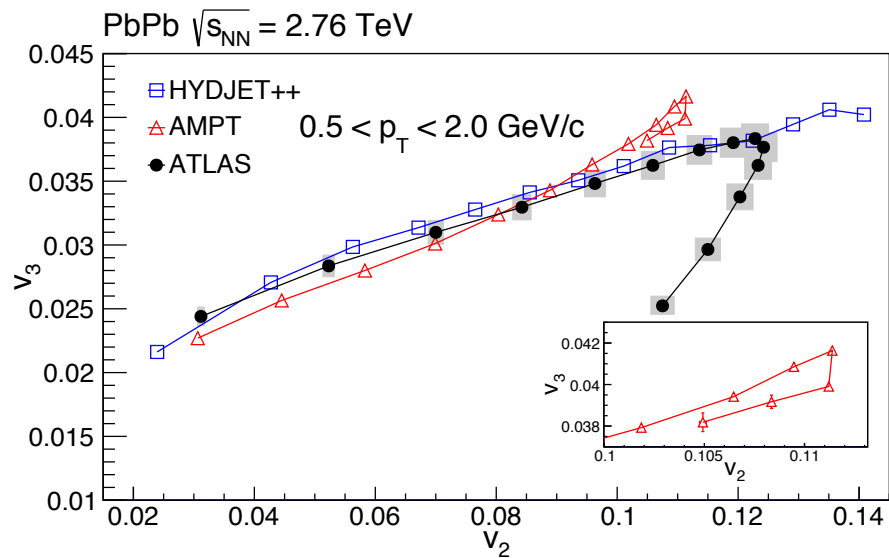
- ❖ The HYDJET++ leading flow mode, $\alpha=1$, essentially equal to the v_3 extracted from two-particle correlations. There is a rather good agreement with the v_3 experimentally measured by ALICE and CMS
- ❖ The sub-leading flow mode, $\alpha=2$, is almost equal to zero \rightarrow the v_3 factorizes much better than the v_2
- ❖ Again, similar behavior wrt the r_3 results (Phys. Rev. C **92** (2015) 034911)

Chin.Phys. C (2017) 074001

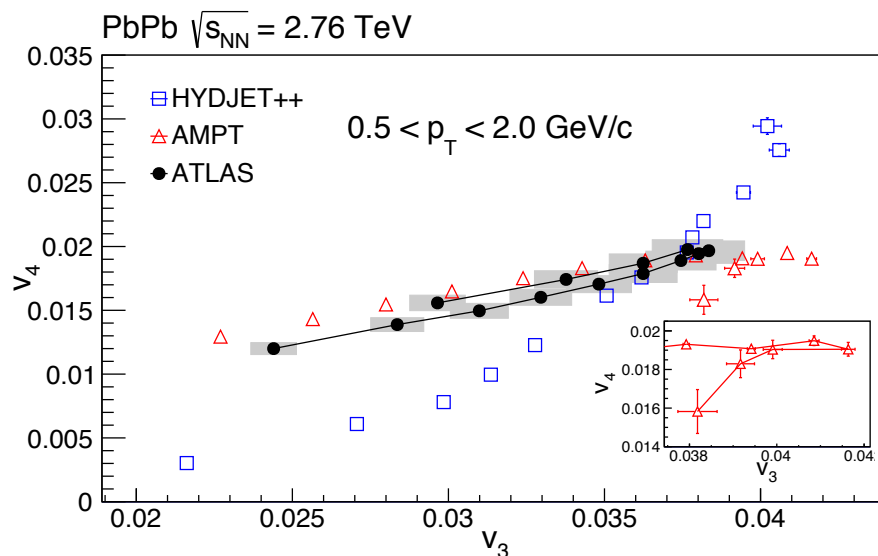
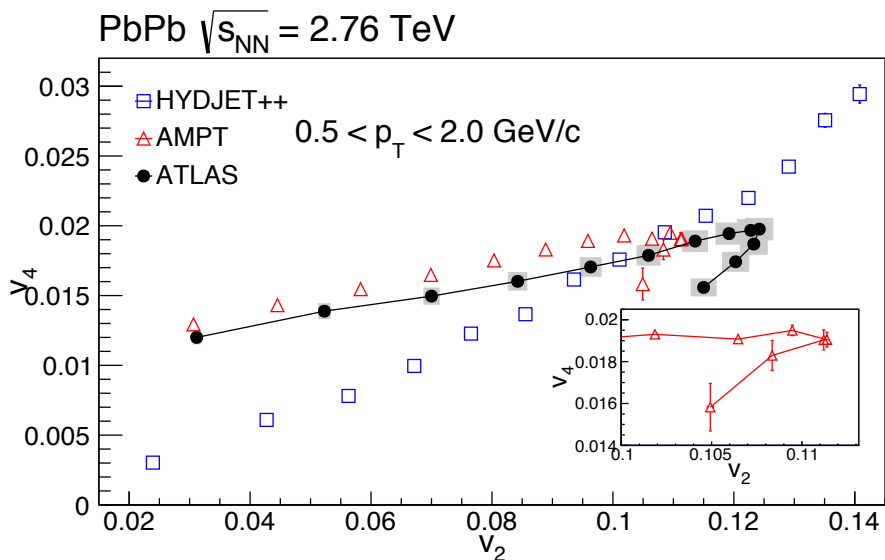
Azimuthal anisotropies and fluctuations from HYDJET++ and AMPT models



v_n-v_m correlations from HYDJET++ and AMPT models



- ❖ For central collisions, both models predict slope of the v_2-v_3 rather well
- ❖ AMPT predicts a boomerang like structure, while HYDJET++ does not
- ❖ AMPT rather well describes v_2-v_4 and v_3-v_4 correlations, while HYDJET++ fails



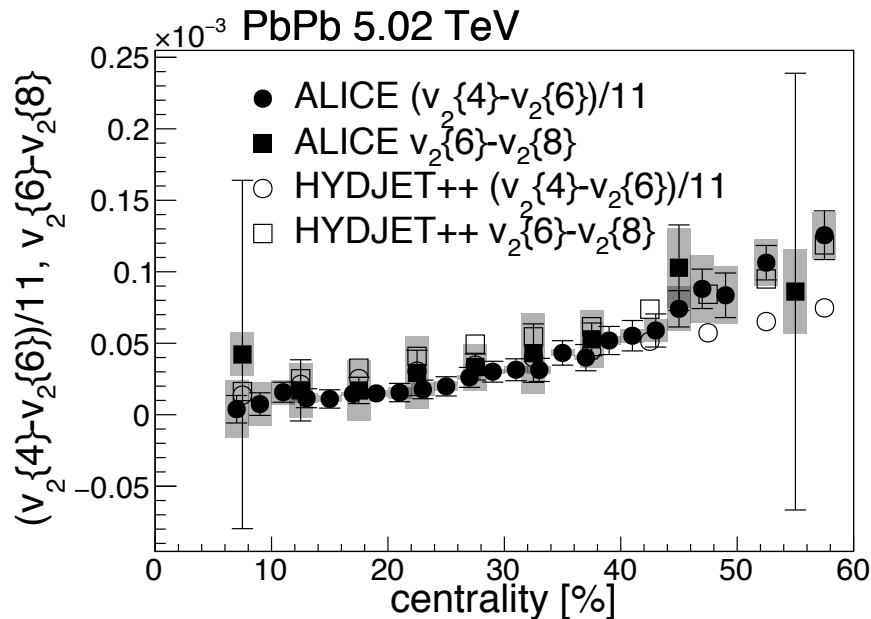
Phys. Rev. C 101 (2020) 014908

ATLAS data PRC 92 (2015) 034903

A hydrodynamics probe and skewness from HYDJET++

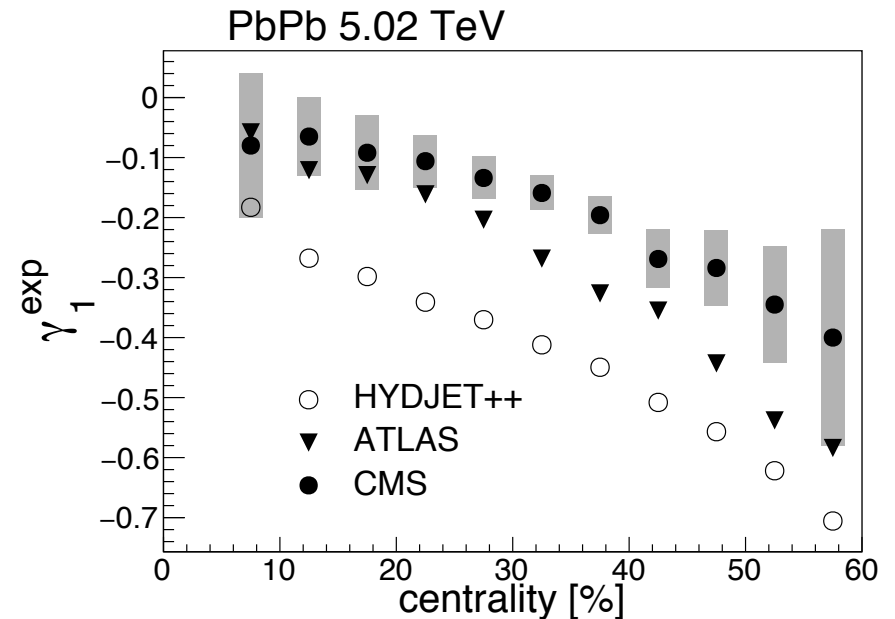
- ❖ If hydrodynamics then universal equality $v_2\{6\}-v_2\{8\} = (v_2\{4\}-v_2\{6\})/11$ is valid
- ❖ A rather good agreement with the ALICE data for $(v_2\{4\}-v_2\{6\})/11$ and $v_2\{6\}-v_2\{8\}$
- ❖ Skewness defined as $\gamma_1^{\text{exp}} = -6\sqrt{2} v_2^2\{4\} (v_2\{4\}-v_2\{6\}) / (v_2^2\{2\}-v_2^2\{4\})^{3/2}$. ISF will produce ordering in higher order cumulant and non-zero skewness
- ❖ Skewness is qualitatively similar to the experimental results, but with stronger magnitudes

ALICE data JHEP **07** (2018) 103



Phys. Rev. C **101** (2020) 034907

ATLAS data JHEP **11** (2013) 183



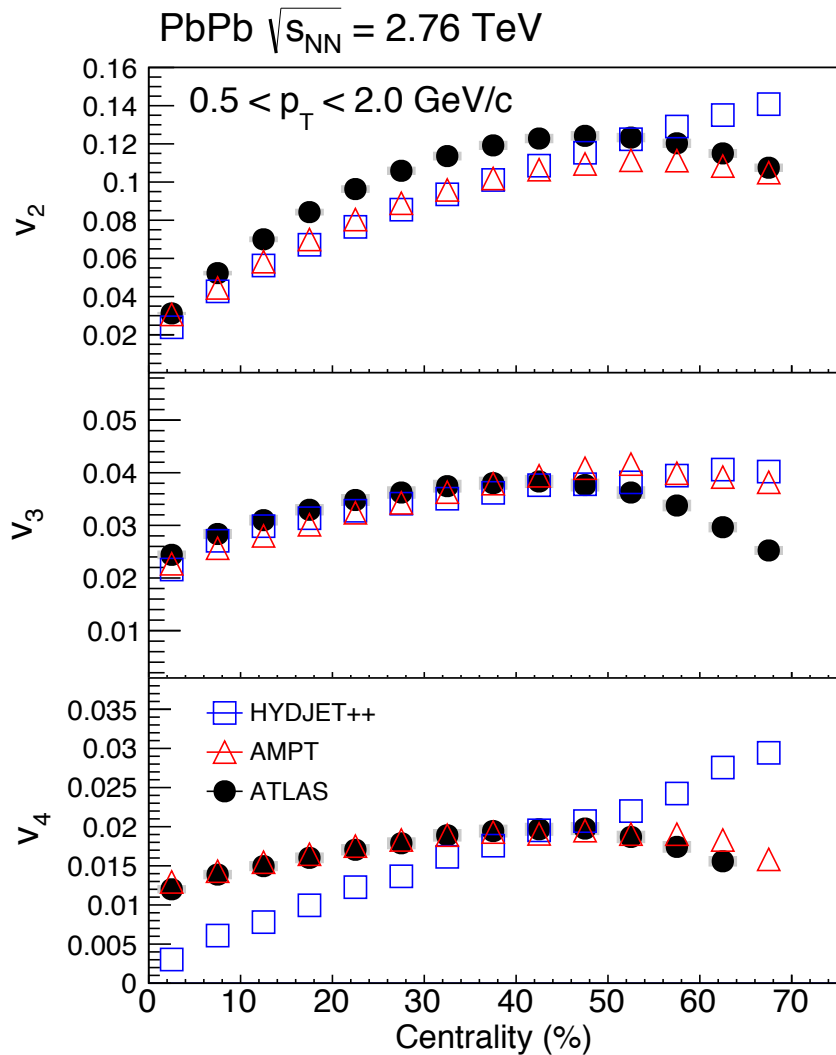
CMS data Phys. Lett. B **789** (2019) 643

Summary

- ❖ The v_2 and v_3 measured at the top SPS energy (CERES)
- ❖ Jet quenching through I_{AA} observable from the ALICE experiment
- ❖ The v_n up to the 7-th order measured in UC PbPb collisions (CMS)
- ❖ The sub-leading v_2 modes qualitatively agree with the r_2 results (CMS)
- ❖ The sub-leading v_3 modes are small if not zero showing that the triangular flow factorizes much better than the elliptic flow (CMS)
- ❖ Subleading flow modes from HYDJET++ are in qualitative agreement with the experimental results
- ❖ AMPT predicts rather well v_n - v_m correlations, including boomerang-like structure, while it is not the case for HYDJET++
- ❖ HYDJET++ predicts rather well $v_n\{2k\}$ cumulants, including ordering of cumulants, hydrodynamics probe and skewness at LHC energy

Backup

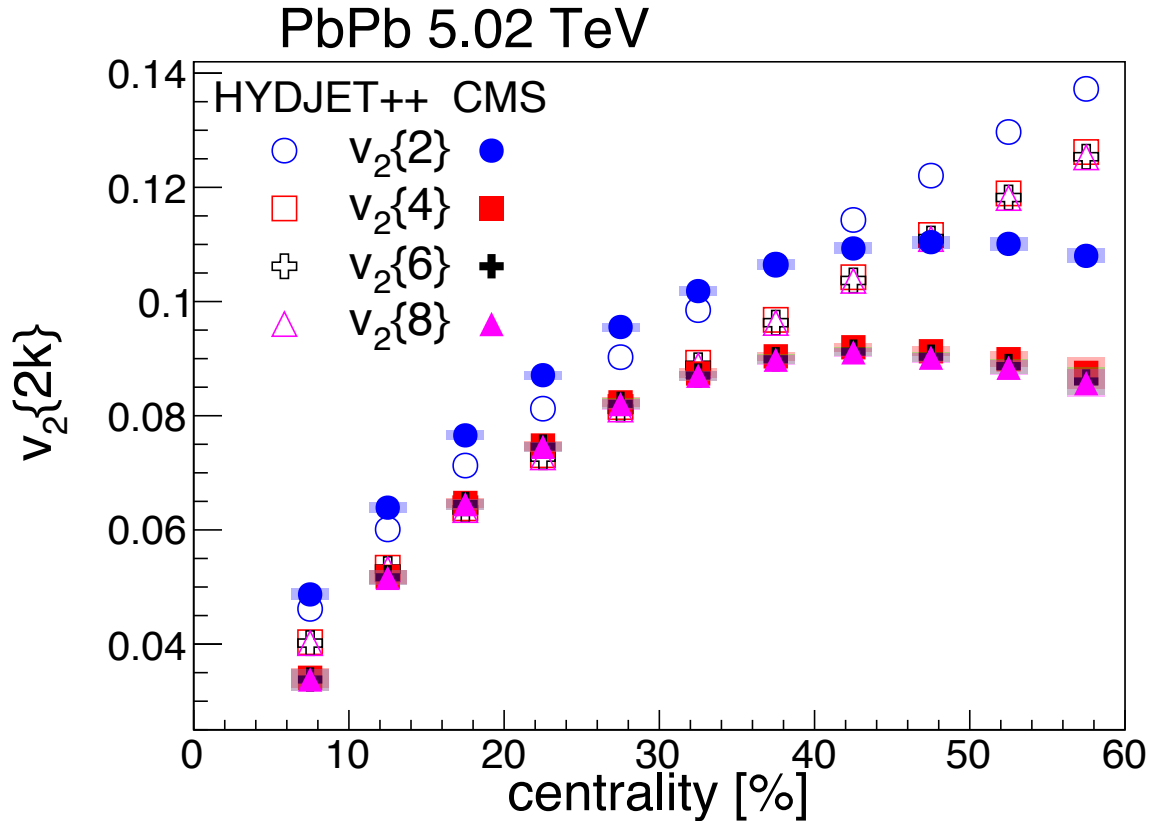
v_n from HYDJET++ and AMPT models



- ❖ Centrality dependence of the v_n harmonics extracted using 2-particle correlation method
- ❖ A good agreement only for v_3 up to 50% centrality for both models
- ❖ AMPT shows a good agreement also for v_4
- ❖ HYDJET++ does not include quadrupole eccentricity – thus badly predicts v_4
- ❖ The results are compared with the ATLAS data taken from Phys. Rev. C **92** (2015) 034903

Phys. Rev. C **101** (2020) 014908

$v_2\{2k\}$ from the CMS and HYDJET++ model



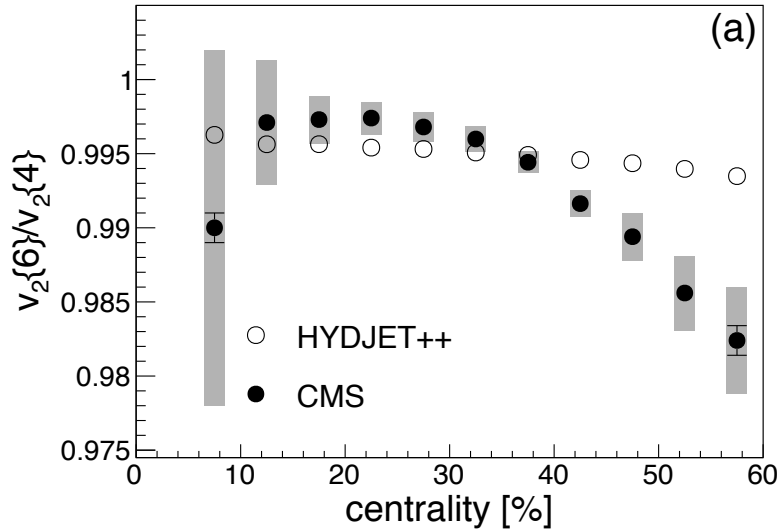
- ❖ In central collisions, HYDJET++ relatively well predicts experimentally measured $v_n\{2k\}$
- ❖ Both, in the experiment and in the model, cumulants are ordered: $v_2\{2\} \geq v_2\{4\} \approx v_2\{6\} \approx v_2\{8\}$
- ❖ In contrast to the experimental data, in peripheral collisions, $v_2\{2k\}$ from HYDJET++ continue to increase

Phys. Rev. C 101 (2020) 034907

CMS data Phys. Lett. B 789 (2019) 643

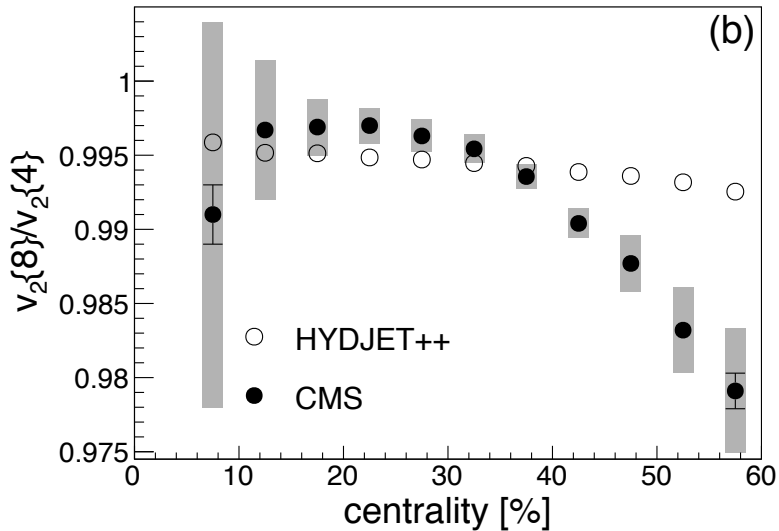
Ratios between cumulants in CMS and HYDJET++

PbPb 5.02 TeV

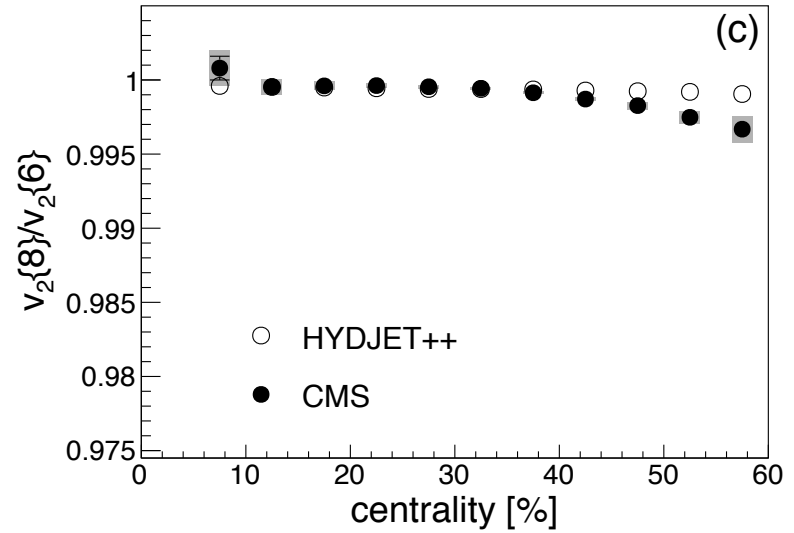


- ❖ HYDJET++ predicts ordering between $v_n\{2k\}$ cumulants
- ❖ The experimental data shows a stronger deviation from unity going to peripheral collisions HYDJET++
- ❖ Overall effect is quite small – less than a promille

PbPb 5.02 TeV



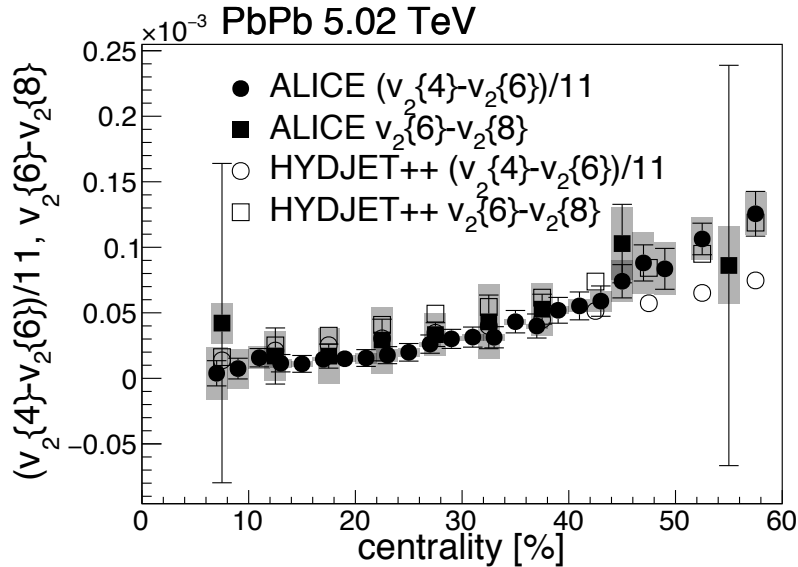
PbPb 5.02 TeV



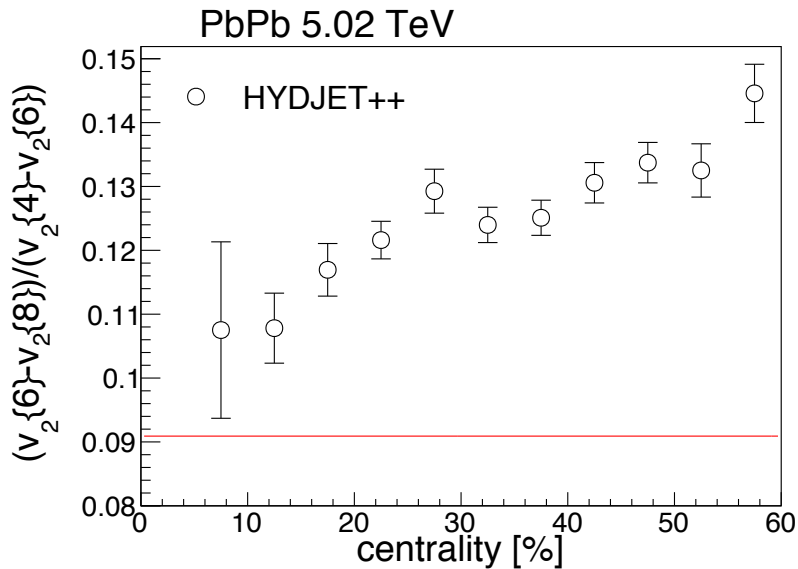
Phys. Rev. C 101 (2020) 034907

CMS data Phys. Lett. B 789 (2019) 643

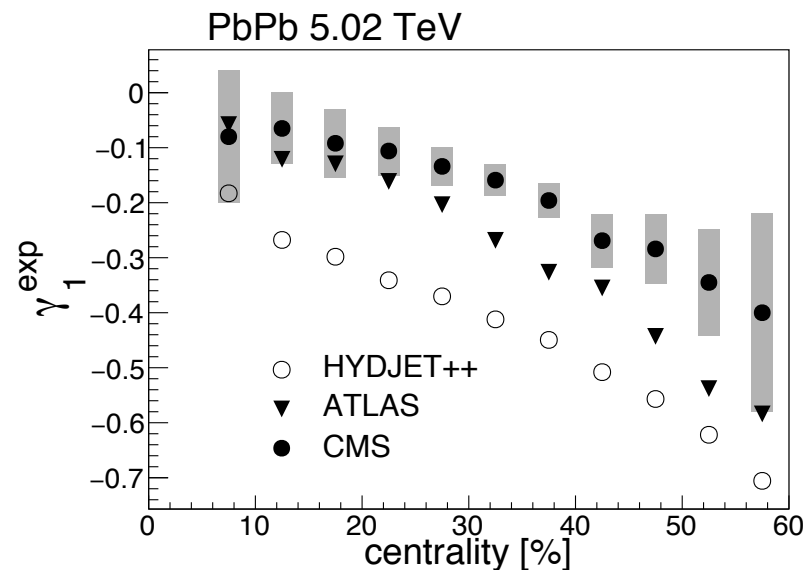
A hydrodynamics probe and skewness from HYDJET++



- ❖ A rather good agreement with the ALICE data for $(v_2\{4}-v_2\{6})/11$ and $v_2\{6}-v_2\{8}$
- ❖ Predicts that the ratio $(v_2\{4}-v_2\{6})/(v_2\{6}-v_2\{8})$ approaches 1/11 going to central collisions
- ❖ Skewness is qualitatively similar to the experimental results, but with stronger magnitudes

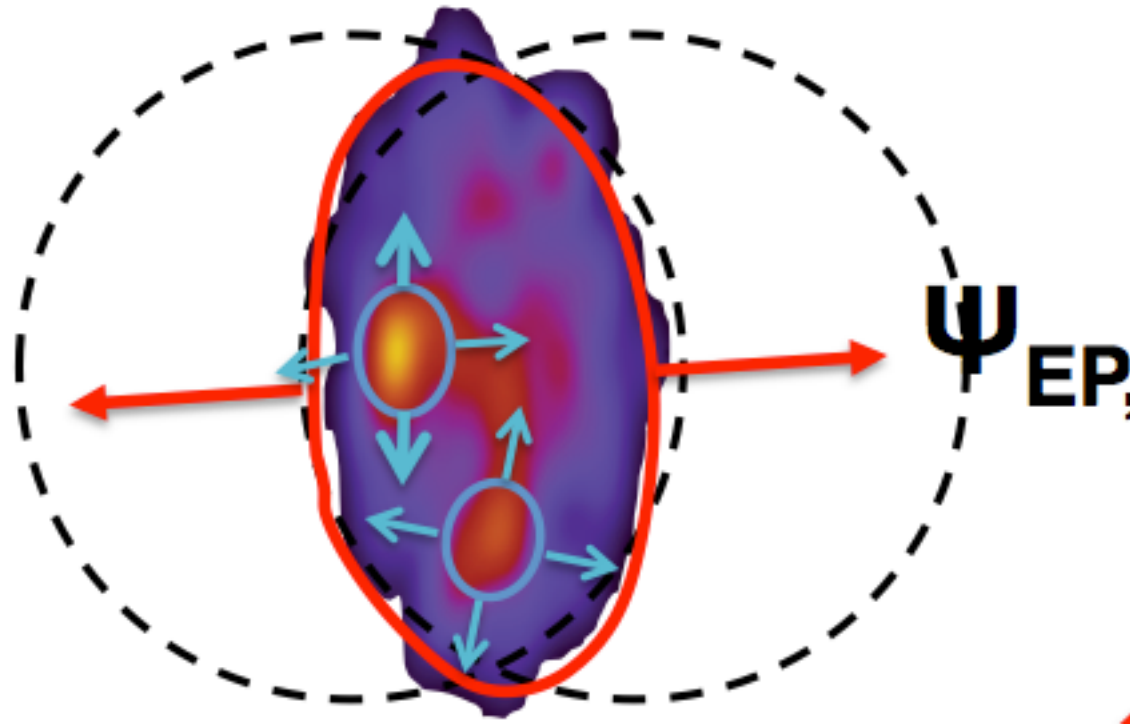


Phys. Rev. C 101 (2020) 034907



CMS data Phys. Lett. B 789 (2019) 643

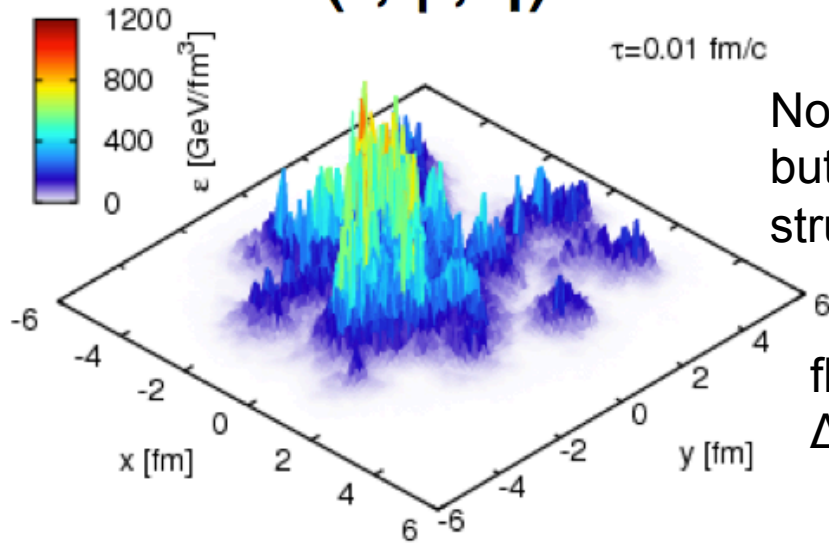
Factorization breaking – p_T and η dependent event plane fluctuations



Initial-state inhomogeneity

Initial state

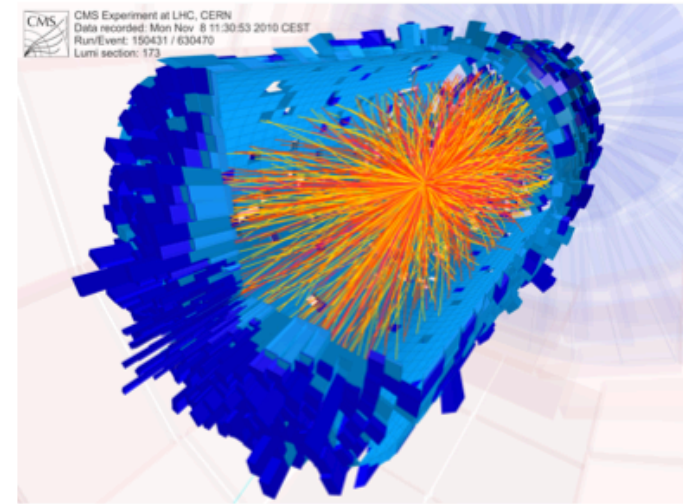
$$\varepsilon(r, \varphi, \eta)$$



EbE hydro.

Final state

$$f(p_T, \varphi, \eta)$$



fluctuations
 $\Delta\varepsilon(r, \phi, \eta)$

overlap zone in x-y

✧ The goal is to map initial-state and its fluctuations in 3D

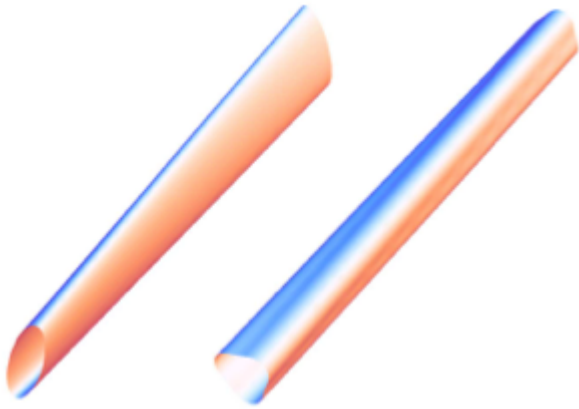
✧ Local hotspots perturb the EP of a smooth medium, so $\Psi_n(p_T)$ contains information about initial-state fluctuations Phys.Rev.C **92** (2015) 034911

✧ Within hydrodynamics, initial-state fluctuations could appear as (sub-leading) flows Phys.Rev.C **96** (2017) 064902

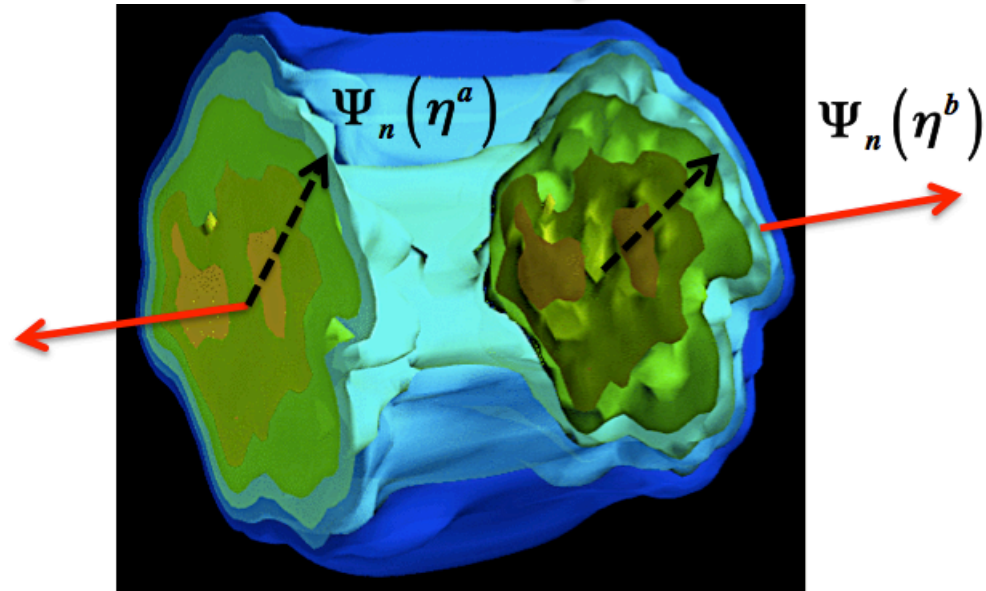
Yesterday, Damir presented in details the dissipation effects in the QGP

Factorization breaking – η dependence

$$f(p_T, \phi, \eta) \sim 1 + 2 \sum_{n=1}^{\infty} v_n(p_T, \eta) \cos[n(\phi - \Psi_n(p_T, \eta))]$$



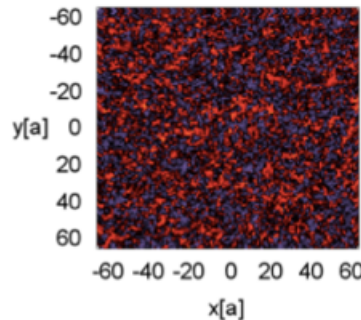
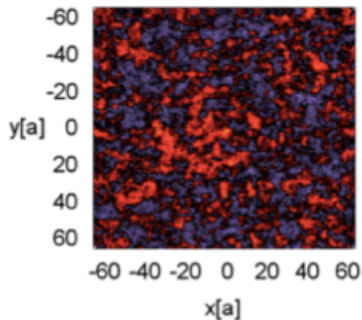
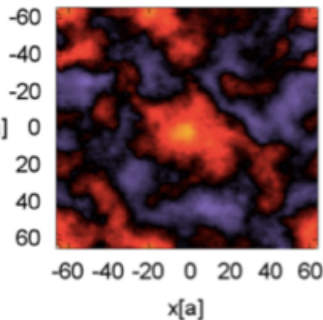
Bozek et al., Phys. Rev. C 83 (2011)034911
Global twist



$Y = 0.0$

$Y = 5.2$

$Y = 10.4$



28.08.2020

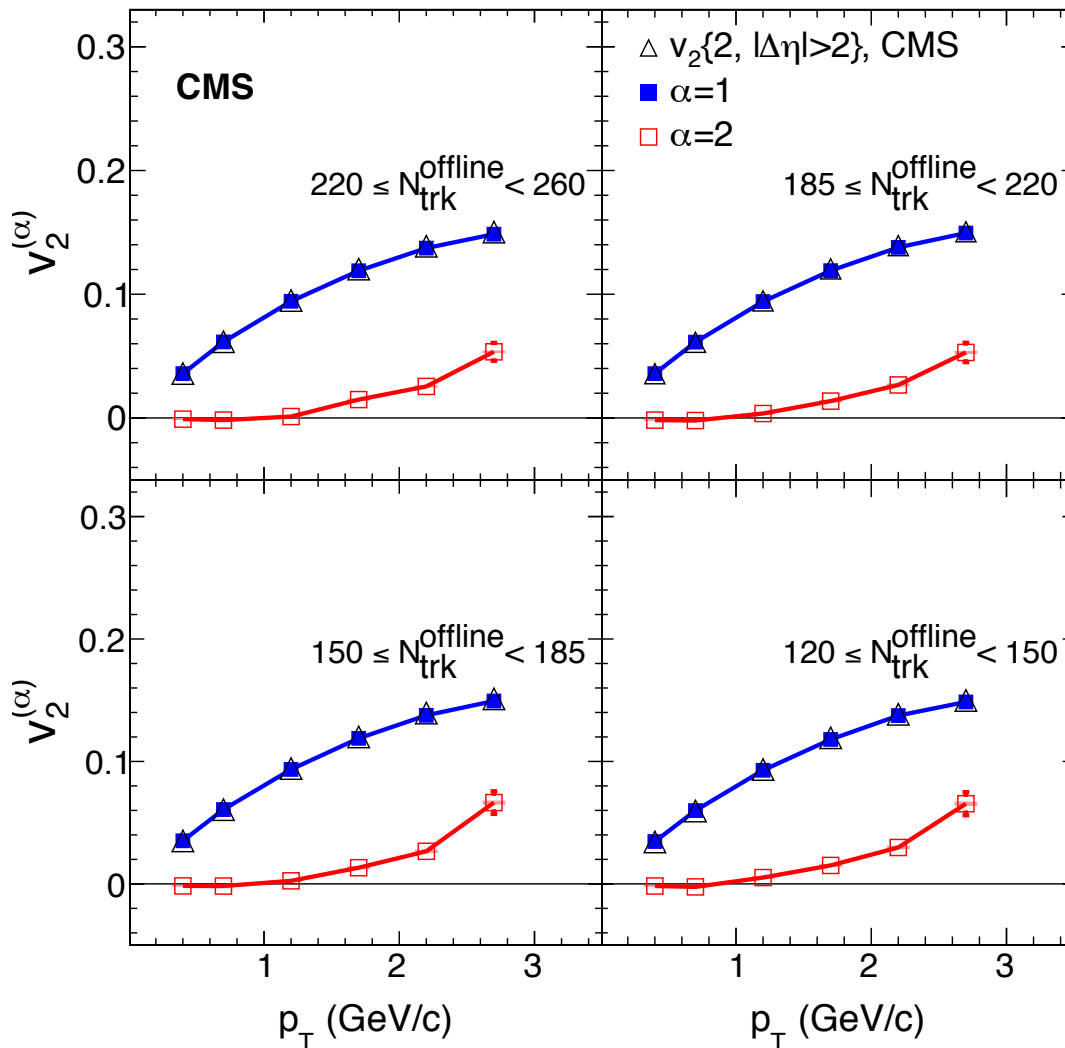
30th SPIG

Dumitru et al.,
Phys. Lett. B 706 (2011) 219

Phys.Rev.C 96 (2017) 064902

Results – elliptic flows in pPb collisions

35 nb⁻¹ (5.02 TeV pPb)

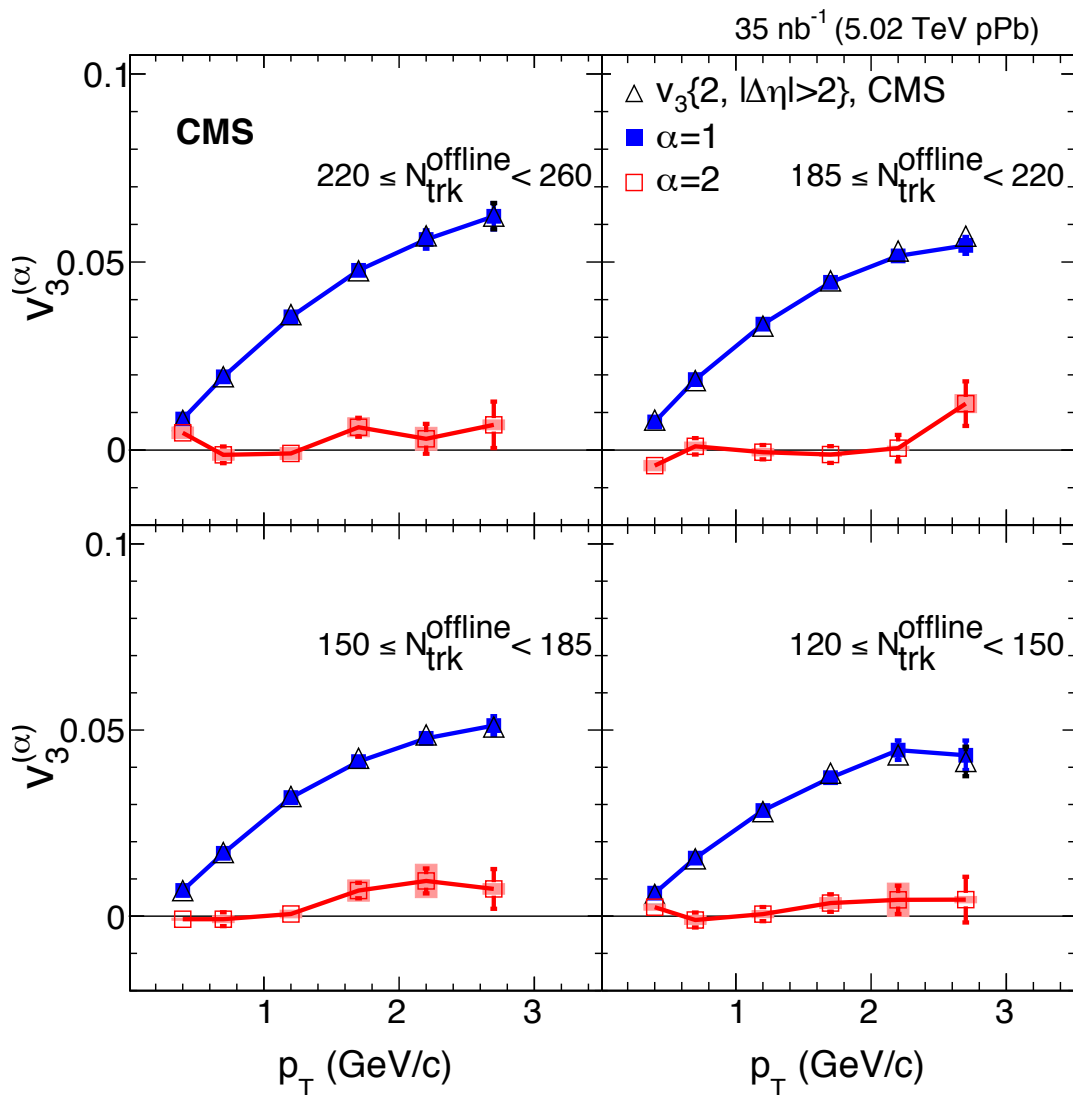


- ❖ The leading flow mode, $\alpha=1$, practically identical to the v_2 measured using two-particle correlations
- ❖ The sub-leading flow mode, $\alpha=2$, is essentially equal to zero at small p_T and increases up to 4-5% going to the high- p_T

Phys. Rev. C 96 (2017) 064902

- ❖ The first experimental measurement of the elliptic sub-leading flow
- ❖ Systematical uncertainties small or comparable to statistical ones only at high- p_T

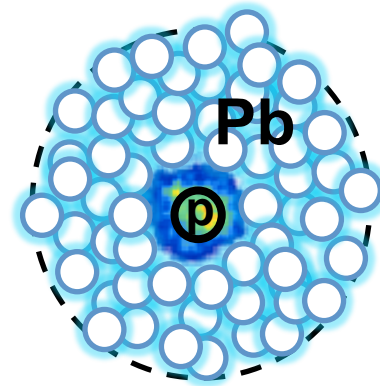
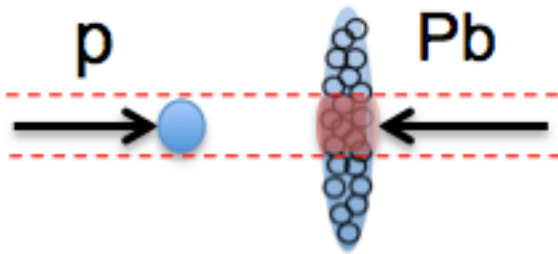
Results – triangular flows in pPb collisions



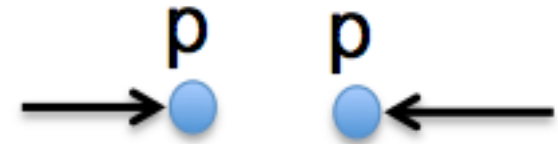
- ❖ The leading triangular flow mode, $\alpha=1$, nearly identical to the v_3 measured using two-particle correlations
- ❖ The sub-leading flow mode, $\alpha=2$, is comparable with zero within the given uncertainties.

Phys. Rev. C 96 (2017) 064902

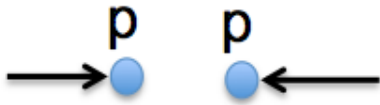
- ❖ The first experimental measurement of the triangular sub-leading flow



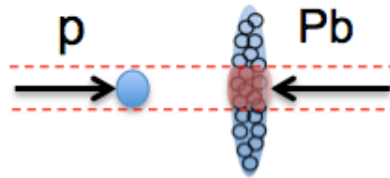
Collectivity in small pPb and smallest pp systems?



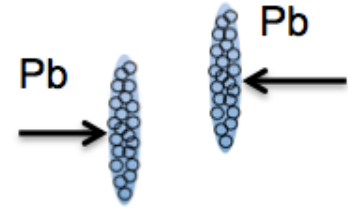
The ridge seen in all colliding systems at LHC



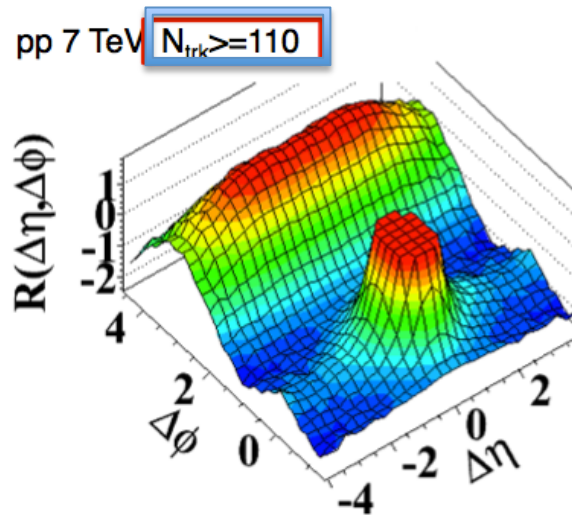
high-multiplicity



high-multiplicity



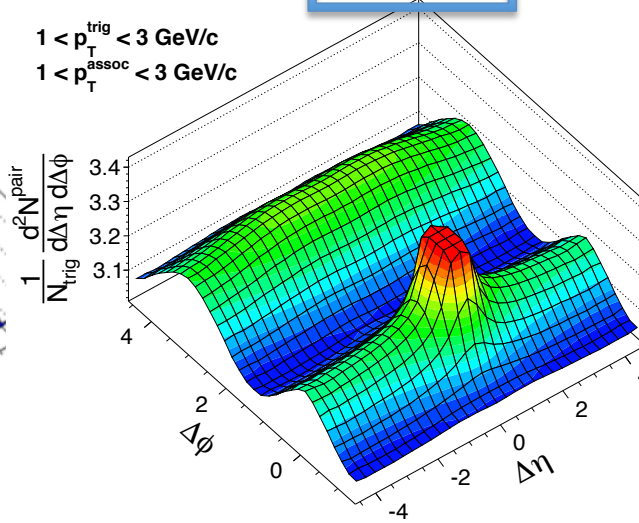
peripheral collisions



JHEP 09 (2010) 091

CMS pPb $\sqrt{s_{NN}} = 5.02$ TeV, $220 \leq N < 260$

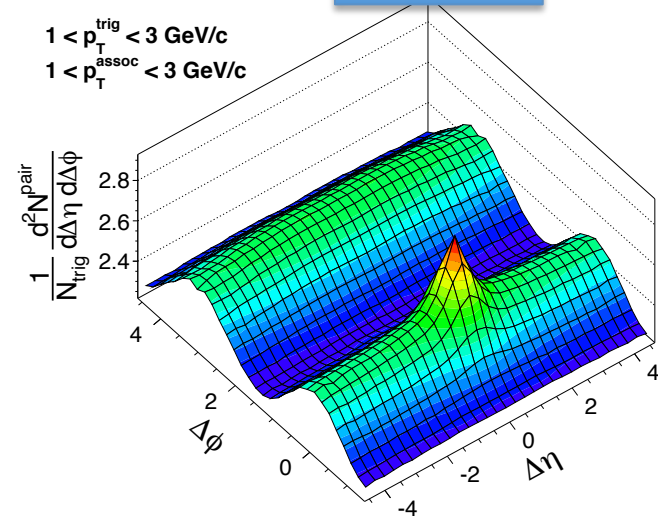
$1 < p_T^{trig} < 3$ GeV/c
 $1 < p_T^{assoc} < 3$ GeV/c



PLB 718 (2013) 795

CMS PbPb $\sqrt{s_{NN}} = 2.76$ TeV, $220 \leq N < 260$

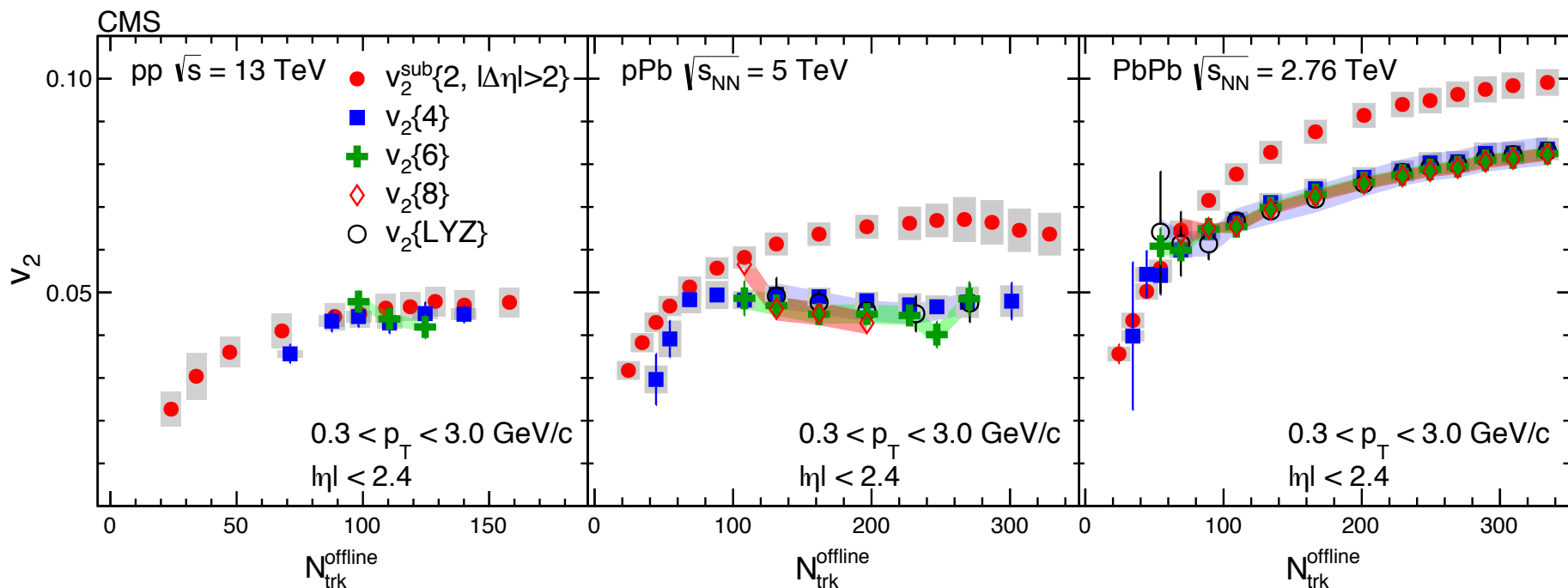
$1 < p_T^{trig} < 3$ GeV/c
 $1 < p_T^{assoc} < 3$ GeV/c



PLB 724 (2013) 213

- ❖ Does the ridge in pp and pPb collisions originate from hydrodynamics flow like in $PbPb$ collisions or it is connected with color-glass condensate (CGC)

v_2 in pp compared to pPb and PbPb results

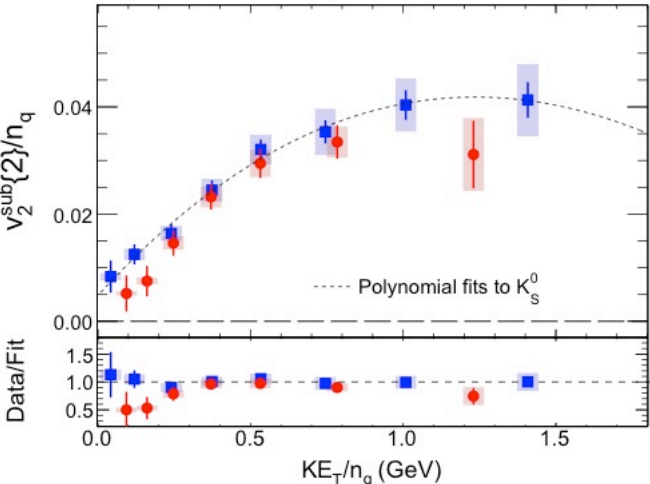
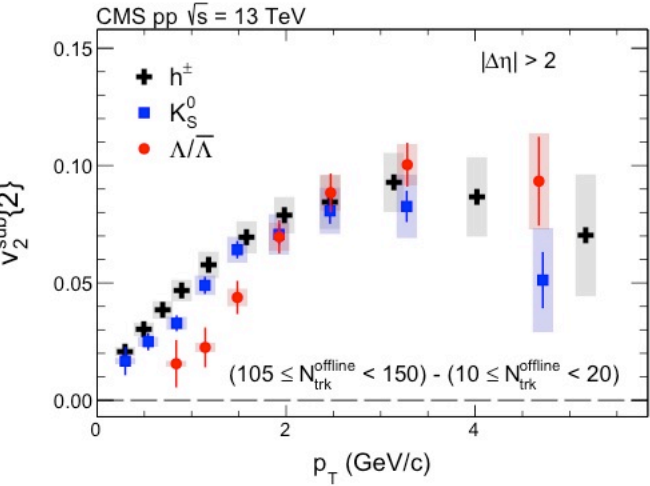


$v_2\{2\} \geq v_2\{4\} \approx v_2\{6\}$
 collectivity!

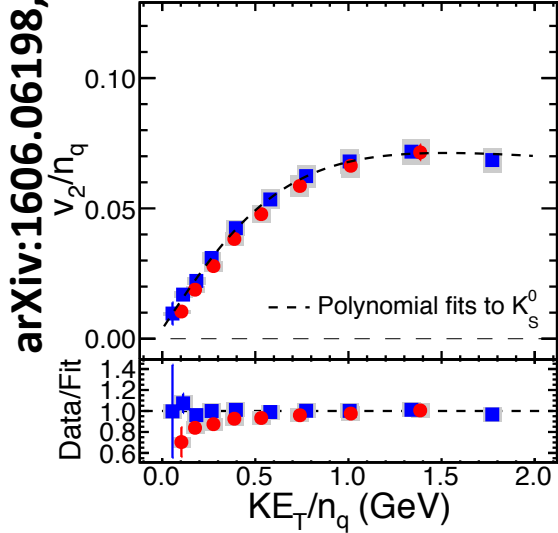
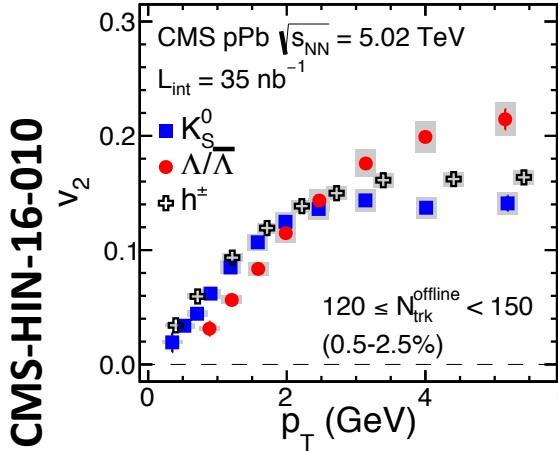
arXiv:1606.06198, CMS-HIN-16-010

- ❖ Elliptic flow in pp measured using 2- and multi-particle correlations – compared to pPb and PbPb results
- ❖ $v_2\{2\}/v_2\{4\}(\text{pp}) \leq v_2\{2\}/v_2\{4\}(\text{pPb}) \leftarrow$ related to initial-state (IS) fluctuations
- ❖ smaller $v_2\{2\}/v_2\{4\} \leftarrow$ less IS fluctuating sources (PRL 112 (2014) 082301)

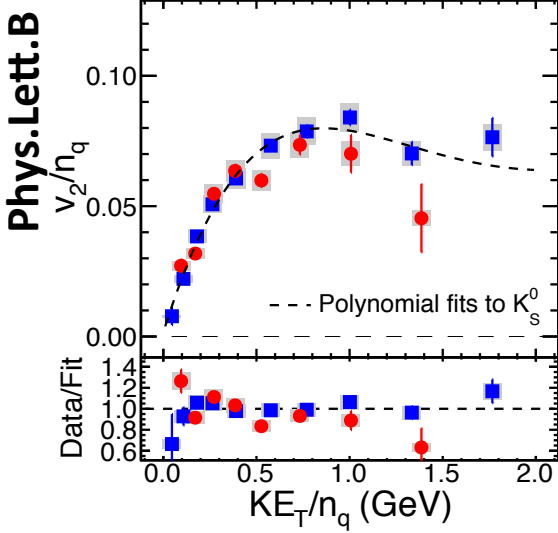
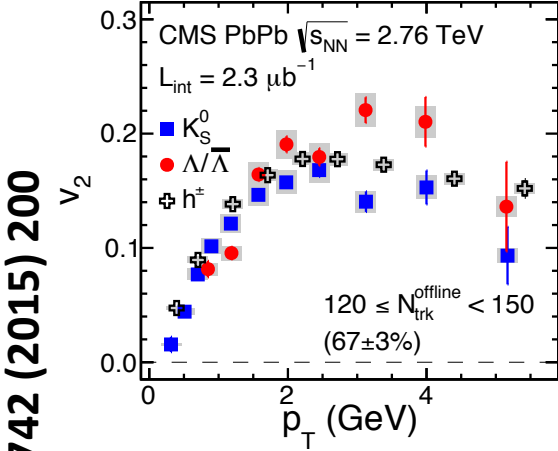
NCQ scaled v_2 in pp collisions compared to pPb and PbPb



collectivity!



arXiv:1606.06198, CMS-HIN-16-010



Phys.Lett.B 742 (2015) 200

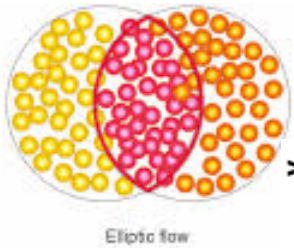
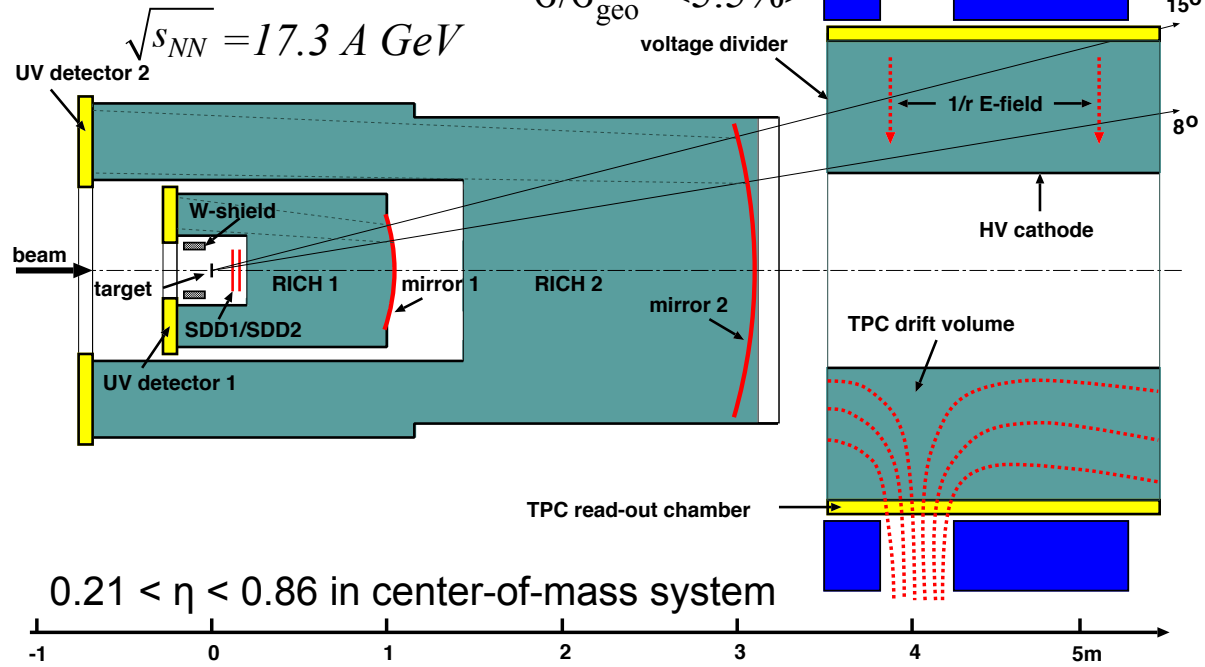
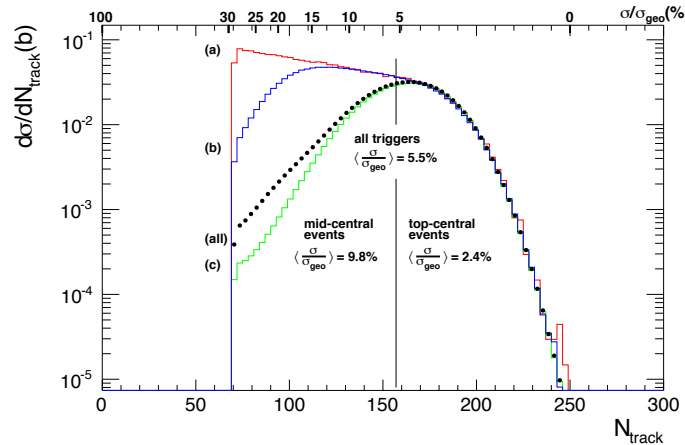
Phys.Lett.B 742 (2015) 200

❖ Significant magnitude of the NCQ scaled v_2 in pp , comparable to the ones seen in pPb and PbPb collisions

Elliptic flow in PbAu at the top SPS energy

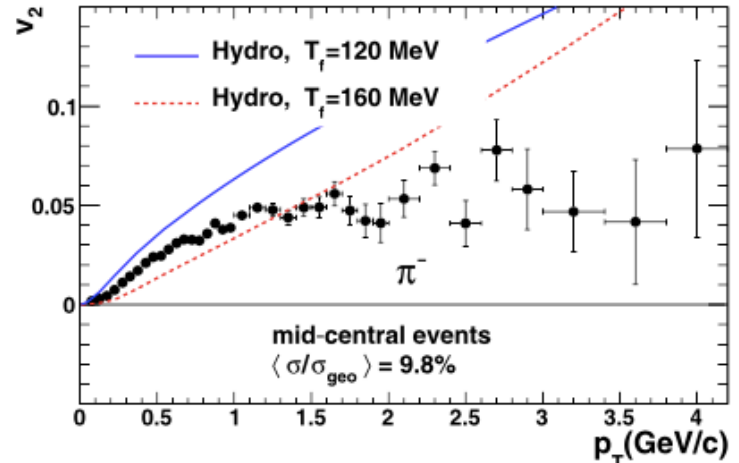
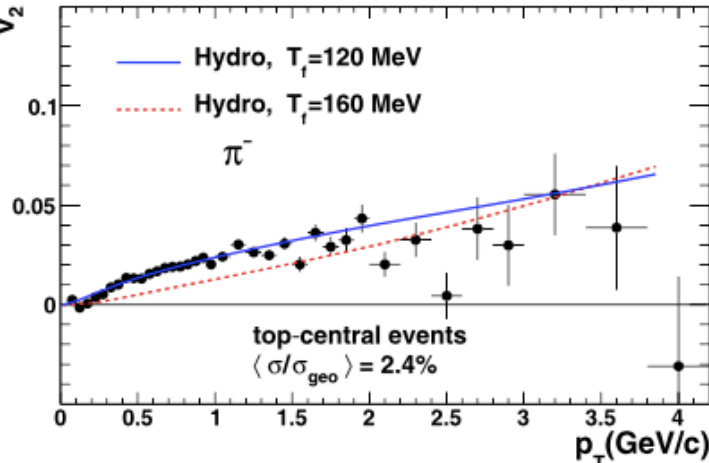
≈30M PbAu collisions collected during 2000 data taking period

mainly central collisions



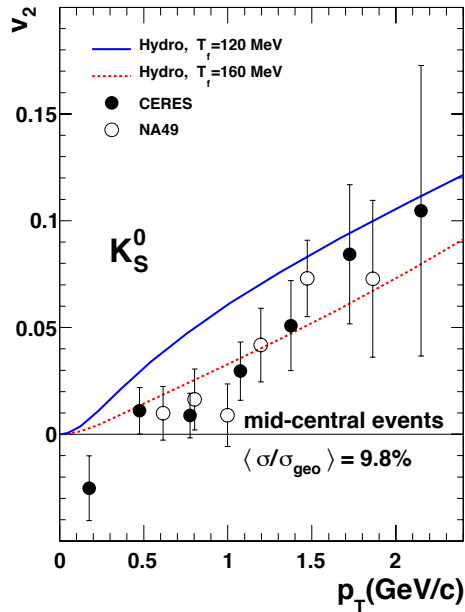
EP method is used

Nucl.Phys.A894 (2012) 41



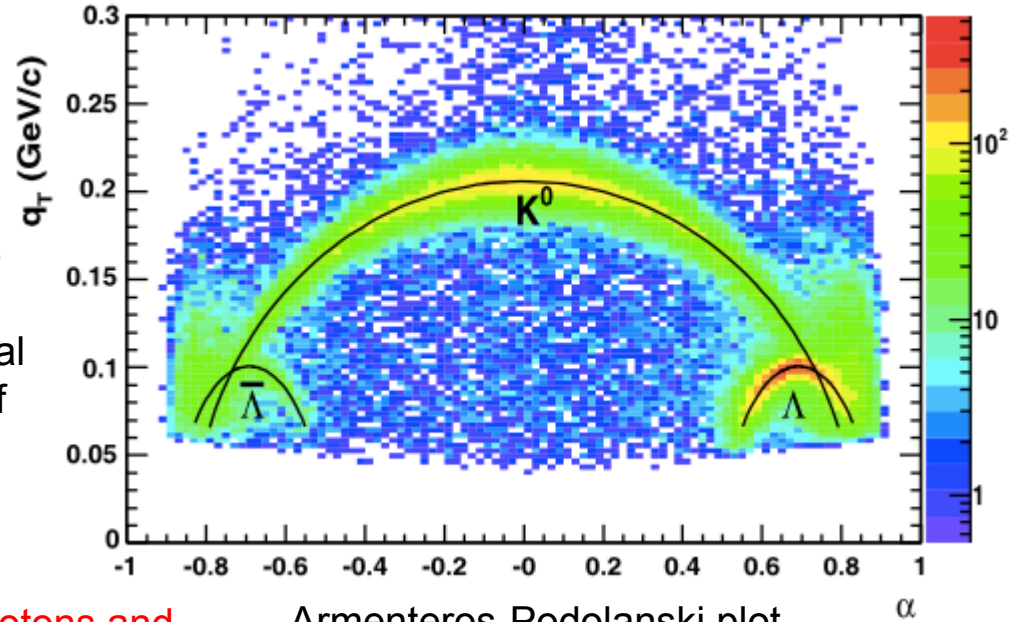
Elliptic flow in PbAu at the top SPS energy

EP method is used



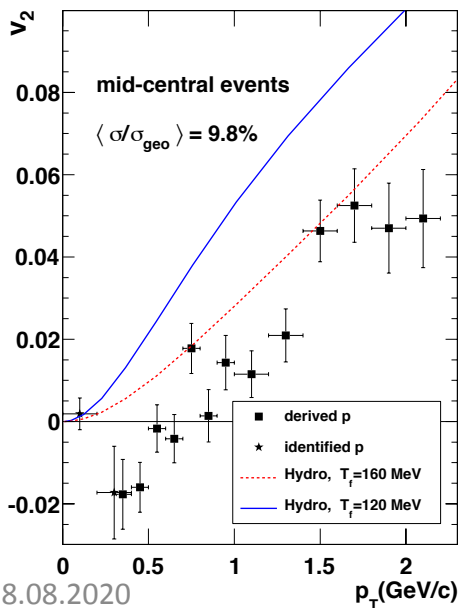
$$\alpha = \frac{q_L^+ - q_L^-}{q_L^+ + q_L^-}$$

q_T and q_L are transversal and longitudinal component of $p_{\Lambda, K} = p^+ + p^-$



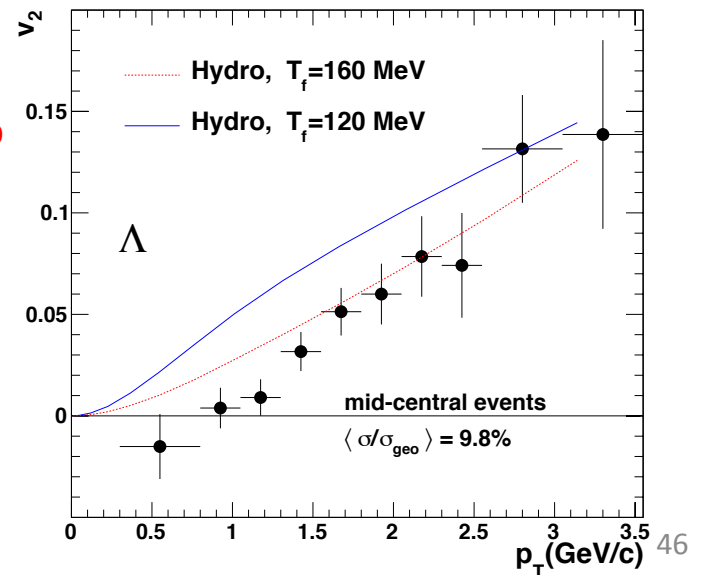
Armenteros-Podolanski plot

Nucl.Phys.A894 (2012) 41



Due to the protons and K^+ admixtures, π^+ sample is not as clean as π^- sample. K^- impurity has a minor effect. That is used to extract proton elliptic flow

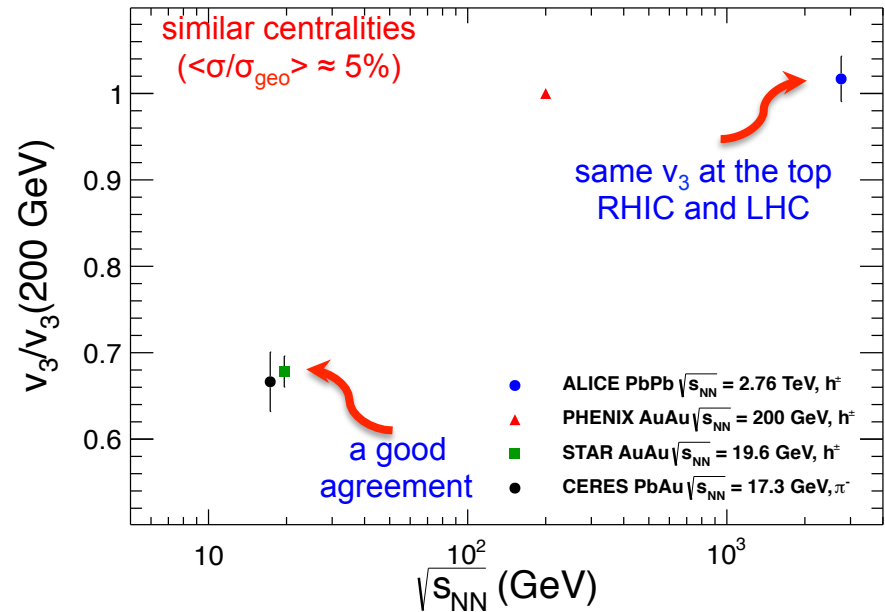
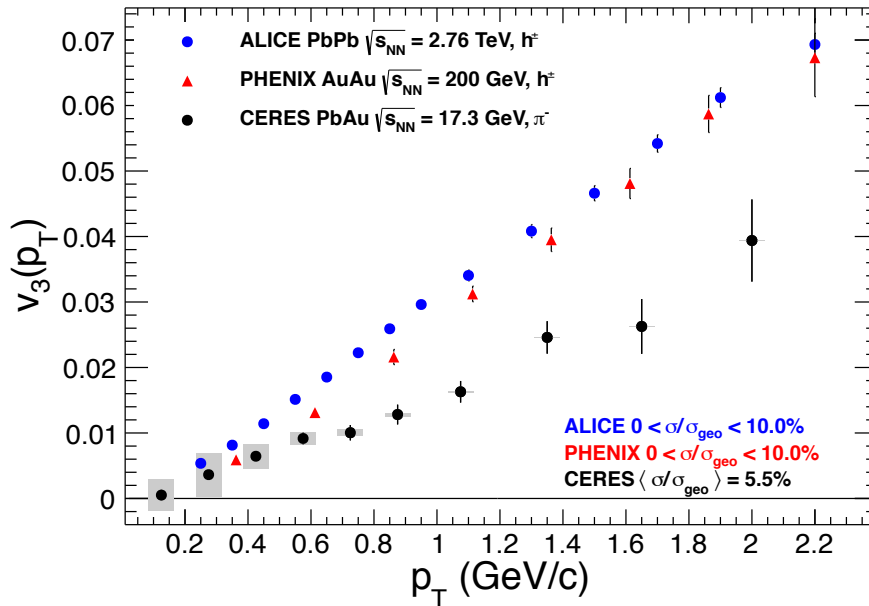
Note a negative baryon elliptic flow around 0.4 GeV/c
3.2 σ below zero



v_3 vs p_T – comparison to other experiments

- ❖ First p_T dependent measurement of the triangular flow at the top SPS energy
- ❖ Top RHIC and LHC energy gives very similar v_3 magnitudes
- ❖ The v_3 at the top SPS energy is about half of those at top RHIC and LHC
- ❖ Linear increase but with different slopes
- ❖ RHIC 19.6 GeV is quite close to the top SPS energy of 17.3 GeV

Nucl.Phys.A957 (2017) 99



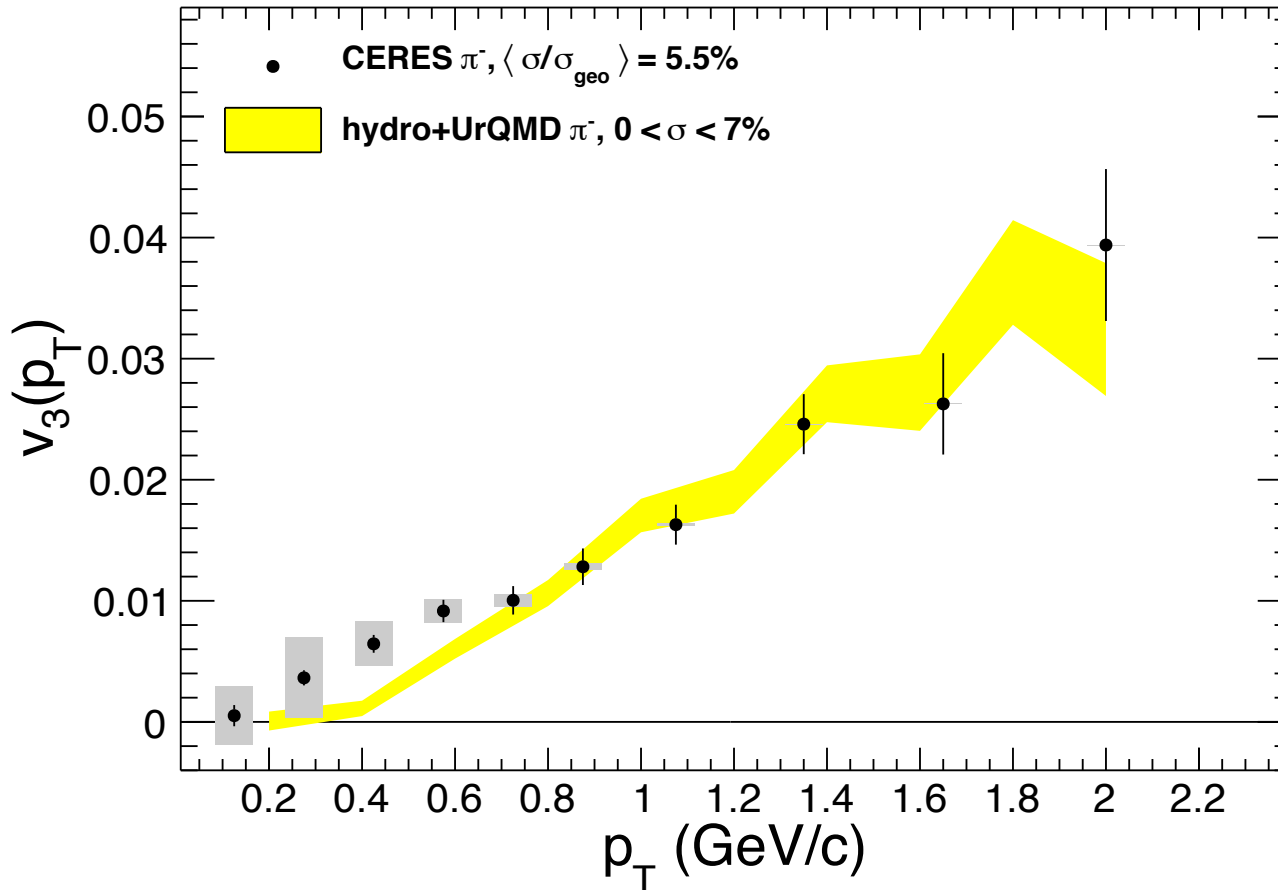
- ✧ As a referent level is taken v_3 value at the top RHIC energy
- ✧ v_3 values integrated over $0.3 < p_T < 2.1$ GeV/c !
- ✧ Note limited p_T range restricted to the CERES acceptance
- ✧ ALICE uses large $|\Delta\eta|$ gaps; No option to include $|\Delta\eta|$ gap at CERES
- ✧ Jet yield is for more than one order of magnitude smaller at SPS

PHENIX
PRL 107 (2011) 252301
 ALICE
PLB 719 (2013) 18
 STAR
PRL 116 (2016) 112302

Comparison with hydro+UrQMD predictions

- ❖ Relativistic hydrodynamics + transport models (hybrid models)
- ✧ vHLLE viscous hydrosolver + UrQMD hadron cascade (I. Karpenko, P. Huovinen, H. Petersen and M. Bleicher **PRC 91 (2015) 064901**)
- ❖ The model predictions for hadrons within $0.2 < p_T < 2.0$ GeV/c and $-1 < \eta < 1$
- ❖ Centrality samples roughly correspond to the experimental ones

Nucl.Phys.A957 (2017) 99



- ✧ Particization at constant energy density 0.5 GeV fm^3
- ✧ Kinetic and chemical freeze-out are dynamical
- ✧ Model predictions in a very good agreement with the CERES results
- ✧ A small disagreement appears at low- p_T

Factorization breaking

- ❖ Assumption that EP angle Ψ_n doesn't depend on p_T leads to factorization

$$V_{n\Delta}(p_{T1}, p_{T2}) = \sqrt{V_{n\Delta}(p_{T1}, p_{T1})} \times \sqrt{V_{n\Delta}(p_{T2}, p_{T2})} = v_n(p_{T1}) \times v_n(p_{T2})$$

- ❖ [Gardim et al., PRC 87 \(2013\) 031901](#) and [Heinz et al., PRC 87 \(2013\) 034913](#)
 Ψ_n could depend on p_T due to event-by-event (EbE) fluctuating initial state

- ❖ then:
$$V_{n\Delta}(p_{T1}, p_{T2}) = \left\langle v_n(p_{T1}) v_n(p_{T2}) \cos \left[n(\Psi_n(p_{T1}) - \Psi_n(p_{T2})) \right] \right\rangle$$

$$\neq \sqrt{V_{n\Delta}(p_{T1}, p_{T1})} \times \sqrt{V_{n\Delta}(p_{T2}, p_{T2})}$$

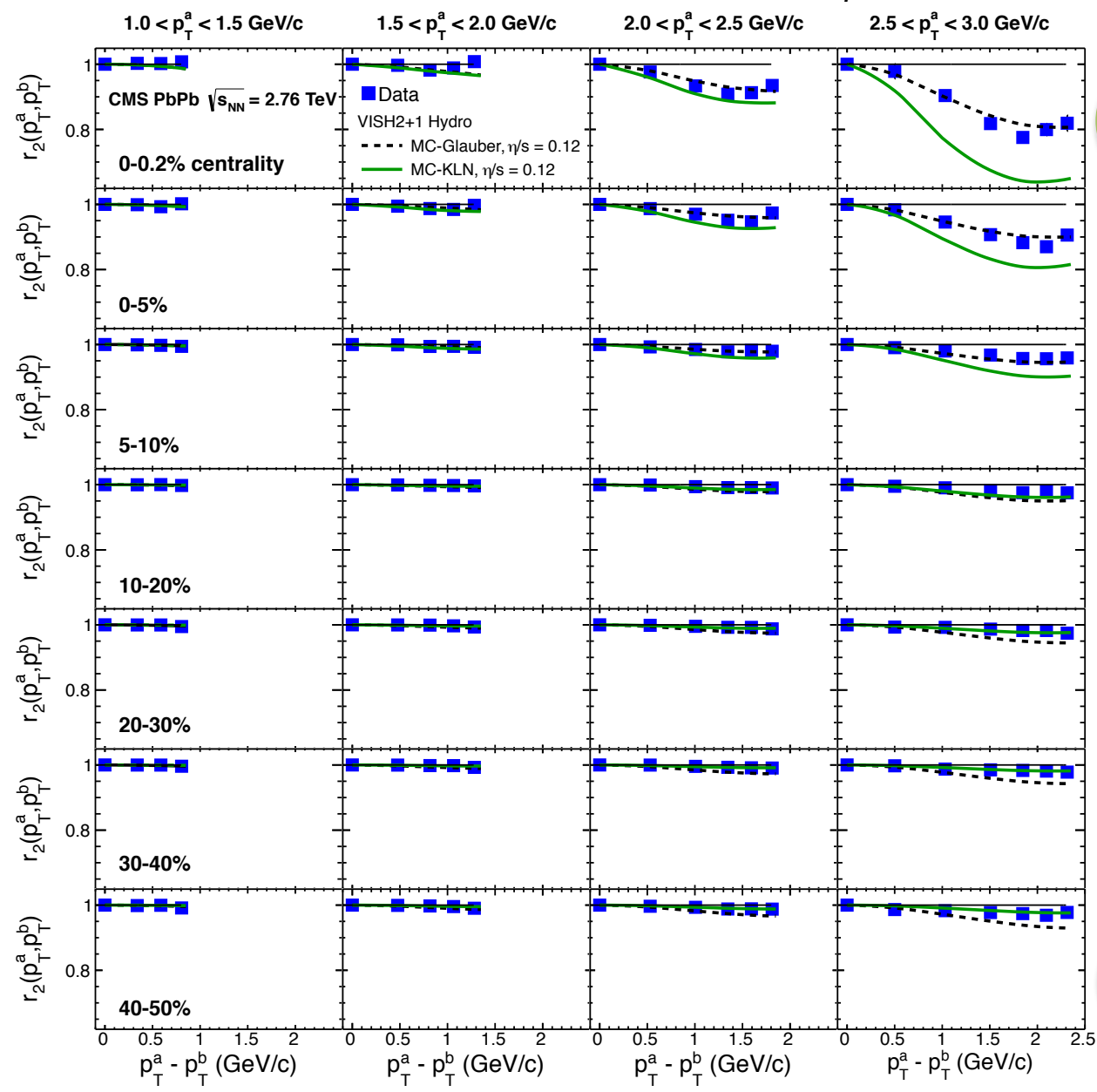
initial state fluctuations $\rightarrow \Psi_n(p_T) \rightarrow$ factorization breaking
 $V_{n\Delta}(p_T^{trig}, p_T^{assoc})$

- ❖ new observable:
$$r_n = \frac{V_{n\Delta}(p_T^{trig}, p_T^{assoc})}{\sqrt{V_{n\Delta}(p_T^{trig}, p_T^{trig})} \sqrt{V_{n\Delta}(p_T^{assoc}, p_T^{assoc})}} =$$

$$\frac{\left\langle v_n(p_T^{trig}) v_n(p_T^{assoc}) \cos \left[n(\Psi_n(p_T^{trig}) - \Psi_n(p_T^{assoc})) \right] \right\rangle}{\sqrt{v_n^2(p_T^{trig})} \sqrt{v_n^2(p_T^{assoc})}} = \begin{cases} 1 & \text{fact. holds} \\ < 1 & \text{fact. breaks} \\ > 1 & \text{non-flow} \end{cases}$$

- ❖ Constraining of initial conditions and η 's by comparing to the exp. data?

→ p_T^{trig}



0-0.2% **PbPb case**



◆ The effect increases with rise of p_T^{trig} and $p_T^{trig} - p_T^{assoc}$

◆ Approaching the central collisions, the effect dramatically increases achieving value over 20%

◆ For semi-central collisions, the effect achieves only a size of 2-3%



40-50%

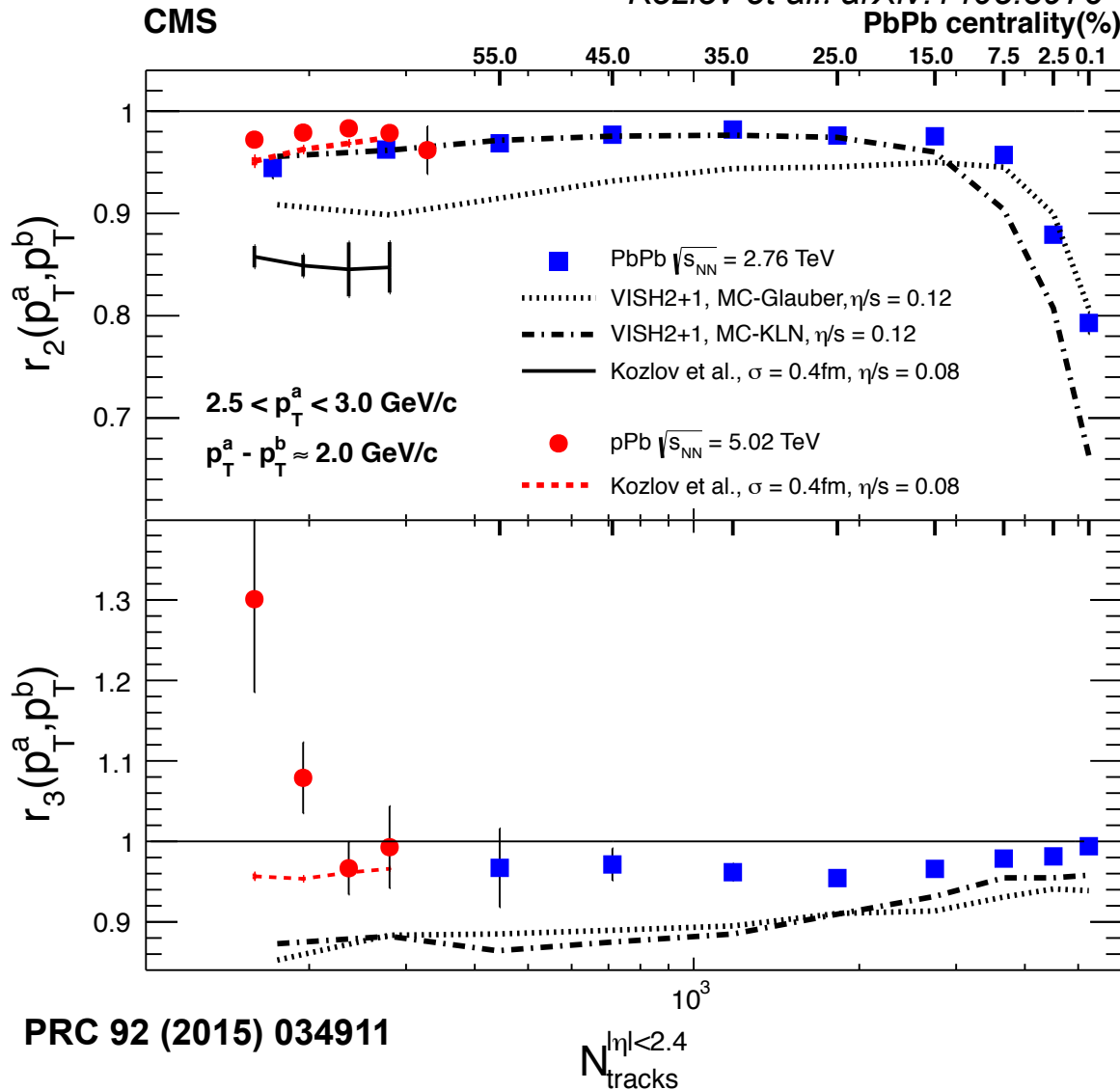


PRC 92 (2015) 034911

r_n multiplicity dependence at the highest Δp_T

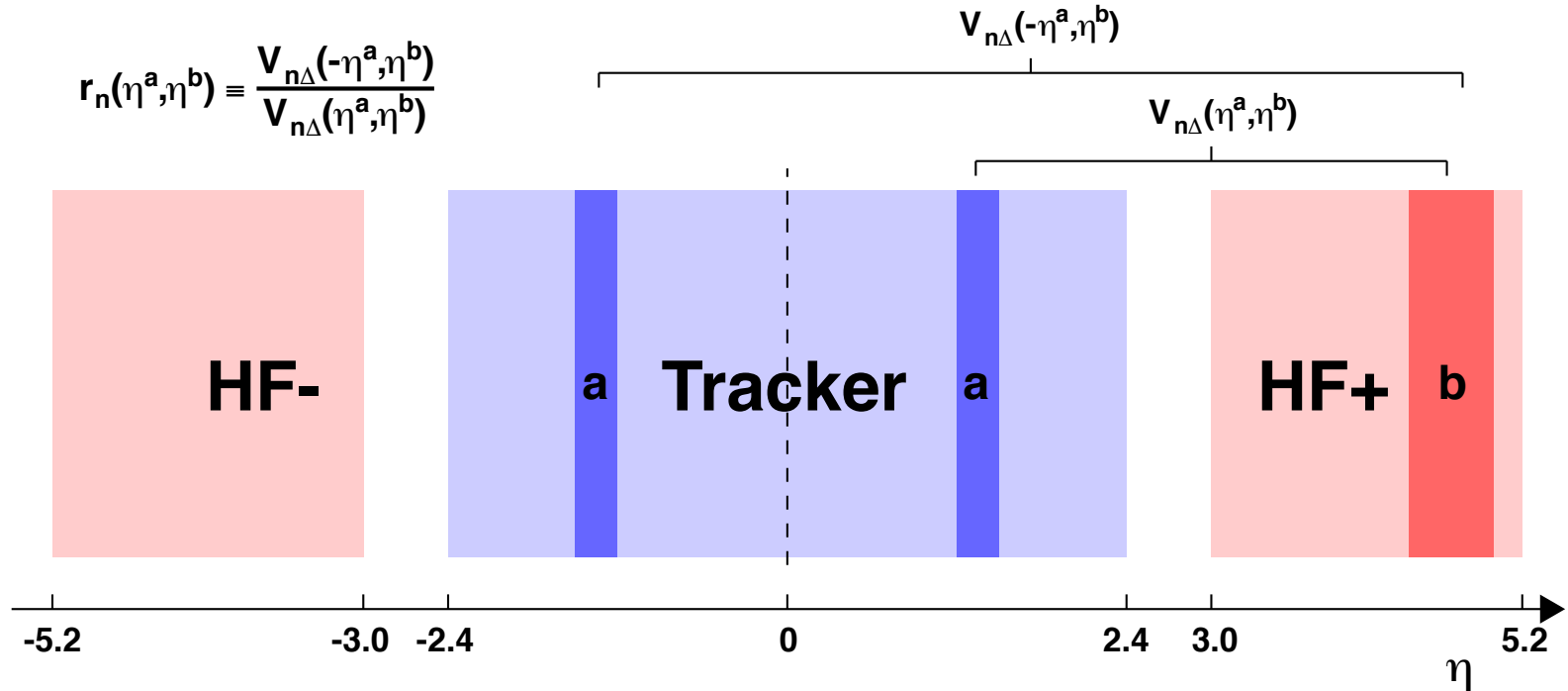
VISH2+1: PRC 87 (2013) 034913

Kozlov et al.: arXiv:1405.3976



- ❖ Dramatic increase at ultra-central PbPb. For small centralities ($>5\%$) \approx few %
- ❖ The r_2 in pPb is a bit smaller than in PbPb
- ❖ Strong r_3 multiplicity dependence in pPb, but very weak in PbPb
- ❖ A non-flow effect in pPb for the highest p_T^{trig} in lower multiplicities
- ❖ VISH2+1 qualitatively describes CMS data
- ❖ Kozlov et al. hydro model describes pPb. Gives stronger effect for PbPb and fails for r_3 at lower multiplicity

η -dependent r_n using Hadronic Forward (HF)



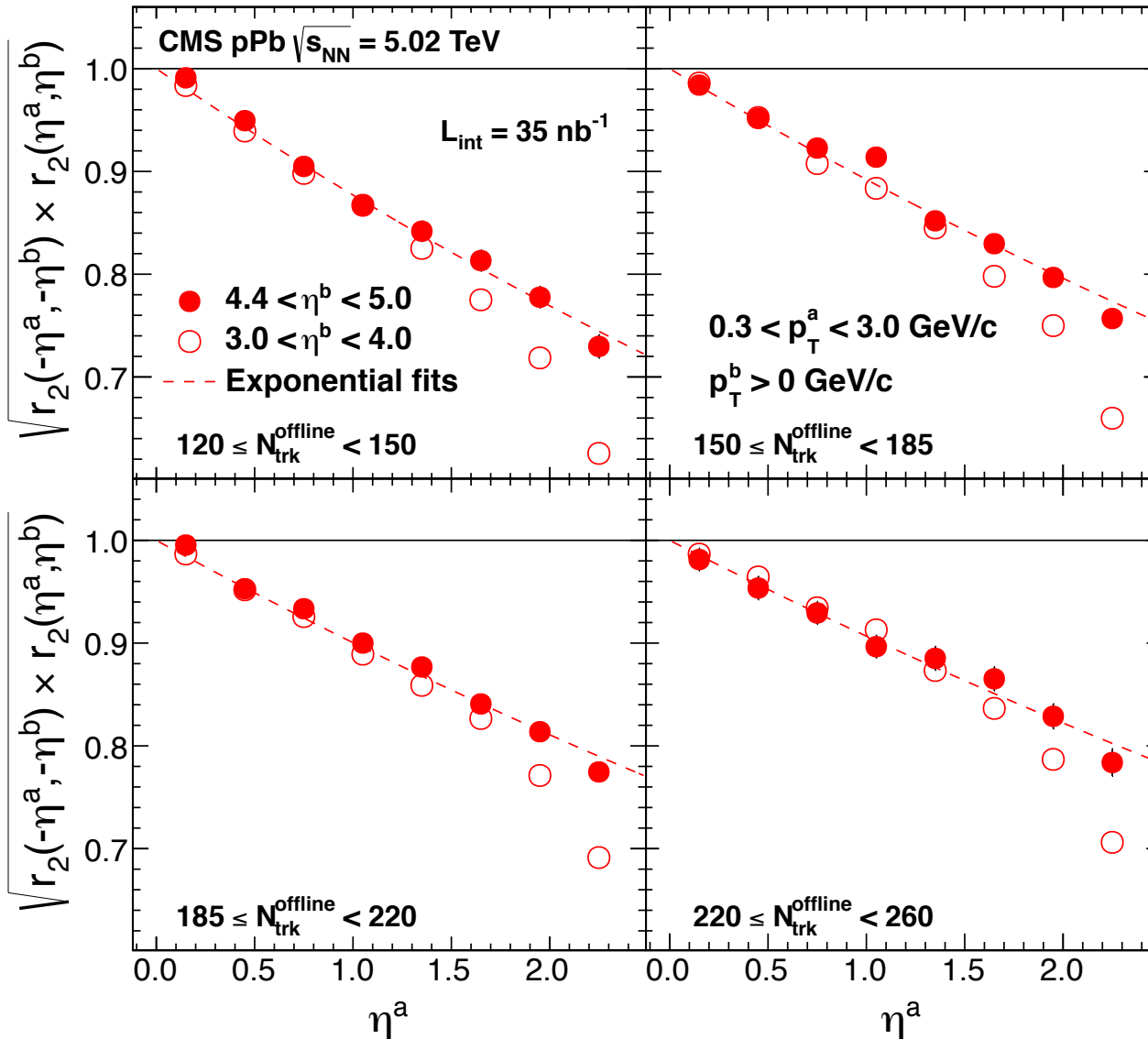
For symmetric collision:

$$r_n(\eta^a, \eta^b) \approx \frac{\langle \cos[n(\Psi_n(-\eta^a) - \Psi_n(\eta^b))] \rangle}{\langle \cos[n(\Psi_n(\eta^a) - \Psi_n(\eta^b))] \rangle}$$

For asymmetric collision:

$$\sqrt{r_n(\eta^a, \eta^b) \times r_n(-\eta^a, -\eta^b)} \approx \sqrt{\frac{\langle \cos[n(\Psi_n(-\eta^a) - \Psi_n(\eta^b))] \rangle \langle \cos[n(\Psi_n(\eta^a) - \Psi_n(-\eta^b))] \rangle}{\langle \cos[n(\Psi_n(\eta^a) - \Psi_n(\eta^b))] \rangle \langle \cos[n(\Psi_n(-\eta^a) - \Psi_n(-\eta^b))] \rangle}}$$

η -dependent r_n in pPb

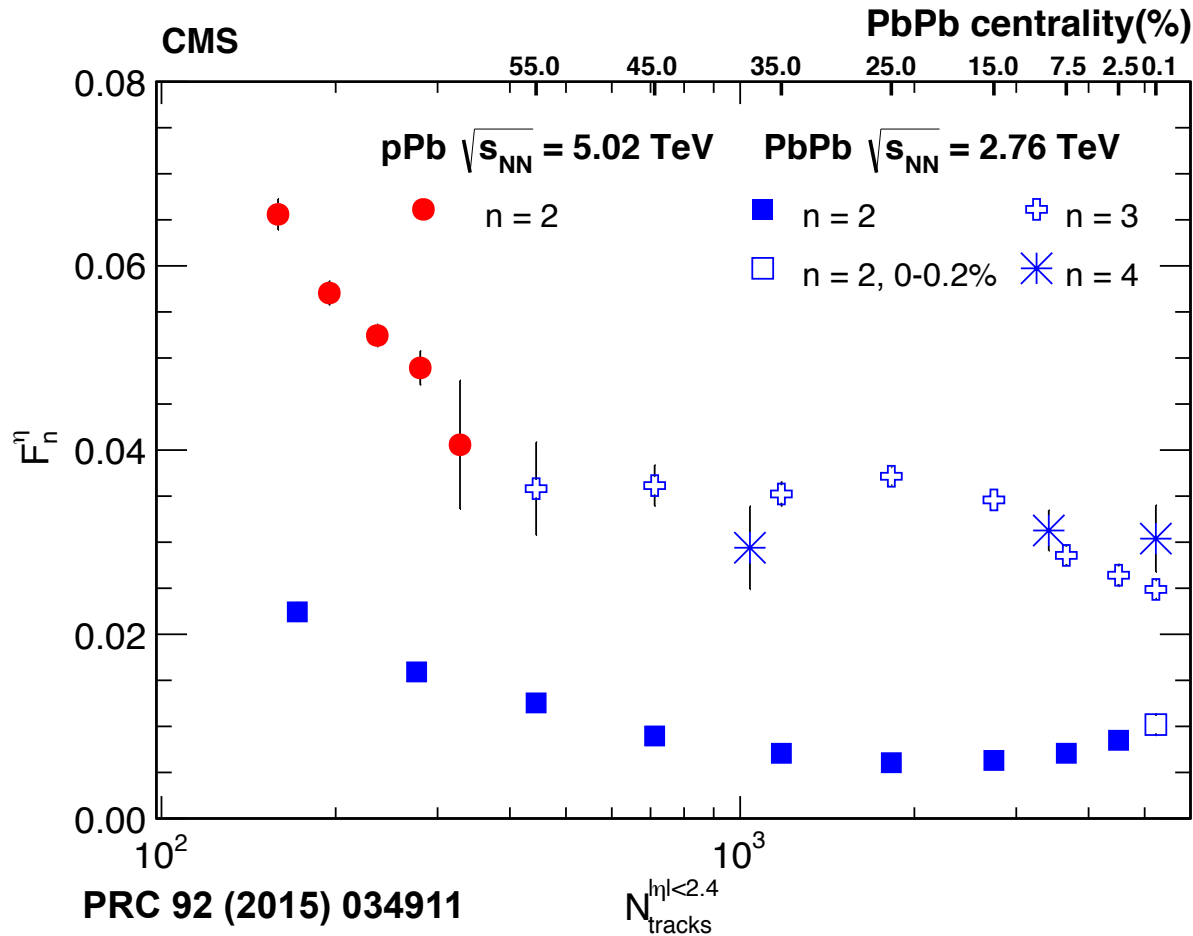


- ❖ A significant factorization breakdown in η found in pPb collisions with increase of η^a
- ❖ The effect increases approximately linearly with η^a
- ❖ Parameterization with F_n^η is purely empirical introduced just to quantify behavior of the data

$$r_n(\eta^a, \eta^b) \approx e^{-2F_n^\eta \eta^a}$$

PRC 92 (2015) 034911

η -dependent r_n vs multiplicity



- ❖ The F_2^η has a minimum around midcentral PbPb and increases for peripheral and most central collisions
- ❖ At similar multiplicity, F_2^η in pPb larger than the one in PbPb
- ❖ Except for the most central PbPb, there is a very weak centrality dependence of F_3^η

- ❖ In PbPb, higher-orders F_3^η and F_4^η , show much stronger factorization breaking than for the second order

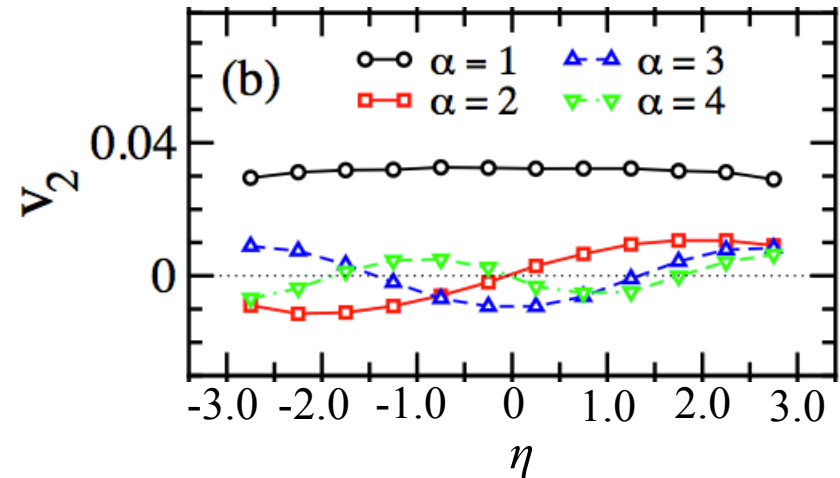
Factorization breaking - connection to the PCA

- ❖ The given harmonic order n has also higher ($\alpha > 2$) eigenmodes ordered from largest to smallest, while in r_n they are not clearly distinguished
- ❖ The PCA can approximately reconstruct two-particle $V_{n\Delta}(p_i, p_j)$ coefficients

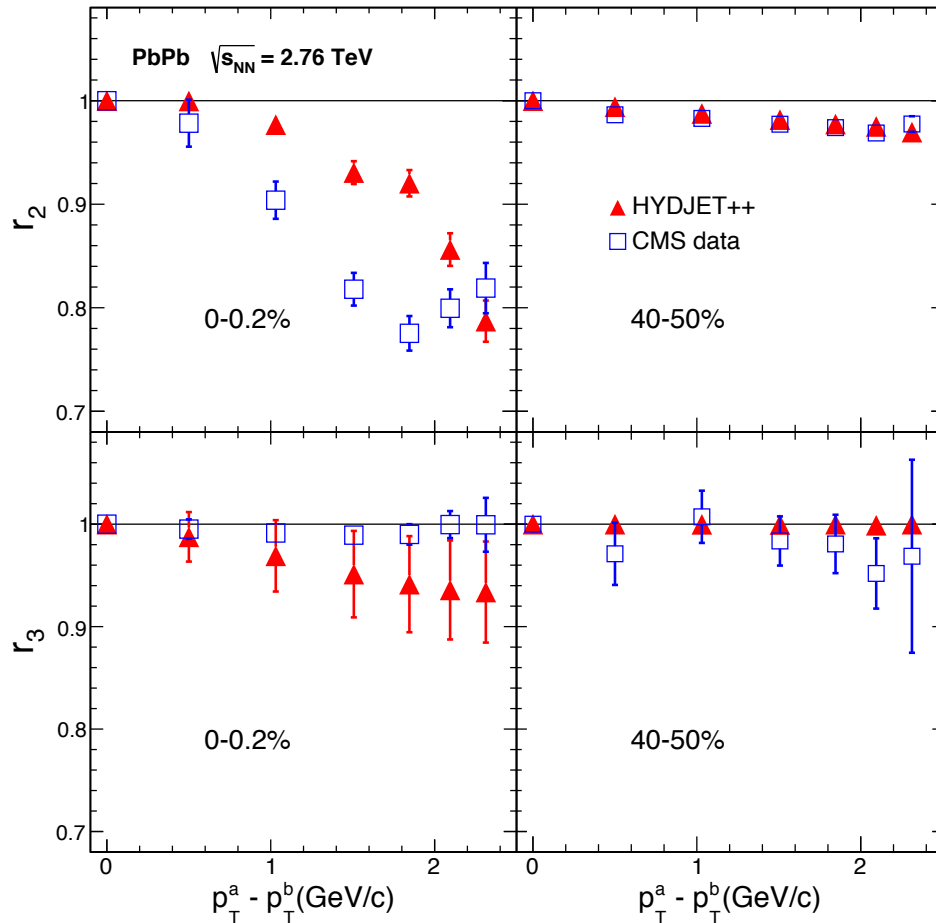
$$V_{n\Delta}(p_i, p_j) \approx \sum_{\alpha=1}^{k \leq N_b} V_n^{(\alpha)*}(p_i) V_n^{(\alpha)*}(p_j) \quad \text{where } N_b = 7$$

which can be used to calculate the factorization breaking ratio r_n

- ❖ So, the PCA is a good tool for analysis in hydrodynamics with fluctuations in the initial state
- ❖ Note that the PCA uses the whole p_T range simultaneously to extract the information on both leading and sub-leading flow modes



Extracted r_n as a function of p_T



$$r_n = \frac{V_{n\Delta}(p_T^a, p_T^b)}{\sqrt{V_{n\Delta}(p_T^a, p_T^a)}\sqrt{V_{n\Delta}(p_T^b, p_T^b)}} \approx \left\langle \cos n(\Psi_n(p_T^a) - \Psi_n(p_T^b)) \right\rangle$$

$$V_{n\Delta}(p_T^a, p_T^b) = \sum_{\alpha=1}^{N_b} V_n^{(\alpha)}(p_T^a) V_n^{(\alpha)*}(p_T^b)$$

- ❖ Pearson coefficients r_n reconstructed from only first two flow modes V_n^α .
- ❖ Qualitatively similar with the experimental r_n in PbPb collisions (Phys. Rev. C 92 (2015) 034911).

Chin.Phys. C (2017) 074001